

Notes for response to review, TCD

Hello Jonathan – hope you are doing well.

I see that TCD requires a mark-up of the original manuscript with annotations of how the revisions and any new contributions were included. Unfortunately, the manuscript underwent several ‘accept all’ stages prior to this final version.

I have provided the final version as a .pdf after the comments below, and the submitted version from 4 June 2014 following that. I think a side-by-side comparison of the texts (perhaps in printed form) will illustrate the changes well.

My apologies for not having a single mark-up to work with.

Best regards,
Ted S.

We thank the two reviewers very much for their comments, and discuss them below. In general we were able to adopt the suggestions completely.

For **Reviewer 1 (H. Rott)**, the main comment was that our combined data sets are overlapping, and not evenly distributed in time or coverage through the period 2001-2010, and so our period of reference for the mass balance assessment is a bit variable within this period. However, the majority of our data are within the 5-year span of higher-quality ICESat data, 2003-2008. We have revised the text to emphasize that, in several places.

Note that in our use of ICESat data we used all possible near-repeat profile pairings available (of those with ~integer-year separations) to smooth out possible short-term variations and to reduce errors (by differencing over multiple years). There is definitely room for future, more detailed studies of year-by-year changes in specific glacier basins, perhaps incorporating airborne altimetry or CryoSat-2 data. Our paper provides a broad assessment of the mass loss rates of the basins for the middle of the decade.

Further comments from **Reviewer 1 (H. Rott)**:

Elevation losses at above 1000 m for the west-flowing glacier basins: We do not see these as contradictory to the ice core data, but rather indicative of even greater loss rates than we measure. The reviewer asks for some indication of the amount of data and the data quality we have for the >1000 m areas of the nAP ridge crest.

To address this, and in part to address the first main comment as well, we are adding a figure to our Supplemental Online Material document that presents the

count of ICESat dH/dt assessments for each of the tracks that we used (new Figure S2). This shows that most of the study area had 3 or more dH/dt assessments from ICESat data.

We state that the data above 1800 meters is not significant because very little area, and therefore very little ICESat data, lie above 1800 meters elevation in the study area. The majority of the high ridge area at 1400-1900 m elevation shows slightly negative to zero elevation change.

On the quoted section of the text ‘...suggests that mass loss rates are not decreasing at this time..’ we were somewhat unclear. Our interpretation of the recent McMillan et al. results using CryoSat-2 data, November 2010- September 2013, is that there is little overall change in the mass loss for the nAP between our study period (centered on 2003-2008) and the most recent estimate (2010-2013). However, a recent paper submitted to GRL by H. Rott and co-authors indicates that the Larsen A embayment is now showing slightly reduced rates of mass loss. We refer to this study (which is likely to be accepted for publication in GRL soon) as ‘personal communication, H. Rott’. We would like to evaluate the Rott manuscript status when our paper is in proof format.

Table S5 references and other issues in the Supplemental Text numbering are fixed now.

Reviewer 2 (N. Barrand) had a series of minor comments which we shall address in sequence. We paraphrase the request or comment below with the reply.

P3238, line 6: Please describe the fraction of the nAP covered by the study

The 33 basin areas represent nearly 100% of the land and ice area shown in Figure 1, which is all the nAP mainland north of 66° S and several of the large nearby offshore islands. The study areas are outlined in white in Figure 1. The only significant land mass not covered within the Figure 1 region is Trinity Island (~100 km²). A few larger islands further northwest of the nAP mainland, for example, Livingston Island and King George Island, are not included. These may have some additional ice mass loss (negative mass balance is likely) that is not counted. We have adjusted the text in the Abstract and Figure 1 caption.

P3238, line 22 Note that the cited past studies do not generally infer processes that are responsible for ice mass loss patterns

Done, with a new sentence in the Introduction

P3239, line 15 Address inexact descriptions of climate-related effects in the study area

Done, by referring to the changes as ‘climate-related changes’ rather than ‘climate change effects’, and other adjustments.

P3239, line 3 What is meant by ‘severe assumptions’ in the Introduction?

Text is changed to 'broad assumptions'. The assumptions were that a regular grid of dH/dt measurements were derived from ICESat track-derived data, and were interpolated to form a complete mapping. This implies that the Antarctic Peninsula is described by a smoothly varying dH/dt field at the scale of 10s of kilometers, whereas in fact there are very large variations in elevation change from basin to basin.

P3239 line 23 Would 'surface elevation change' be a better word choice than 'vertical movement'

Done, and the correction for 'the' Advanced Spaceborne.. is also done.

P3240, line 6 and elsewhere Address the multiple periods of elevation change measurement

This was also mentioned by Reviewer 1 (H. Rott). Because of the overlap of the ICESat data period, and the use of multiple laser campaign pairs for a given ICESat track site, the best detail we can provide for our assessment is 'centered on the period of the highest-accuracy ICESat data, September 2003 – March 2008'. All available estimates were combined, from both dDEM dH/dt data and from ICESat profile comparisons. We have adjusted the text in several places to emphasize this, and in Table 1 and Table S2.

P3240 line 16 Suggest change 'to migrate the measurement track data..'

Done

P3241 line 2 Suggest labeling islands and other features in Figure 1

In fact, Figure 1 is intended as a locator map for the measurement basins, and the names in the figure refer to the Table S2 entries. Addition of further place names would only complicate this figure further. We believe the Figure is more useful as it is. The only islands not clearly named (but instead are abbreviated) are James Ross Island, Dundee Island, and D'Urville Island. These names are spelled out in the Table 1 and 2 (and S2, S3) footnotes. No changes were made to Figure 1.

P3241 line 18 Provide map of ICESat data locations

This is now provided as Figure S2. Note, however, that ICESat data are only mildly weighted relative to dDEM data, because of the very large number of grid cells for each dDEM. As noted in the text, the idea was to allow ICESat data to have some impact in regions where nearly zero dDEM data exist. In any region where dDEM coverage is spatially continuous, these data dominate the assessment.

P3241 line23 Address the multiple periods of elevation change measurement (again), and discuss our assumptions for the ice-front-loss estimates

This is now addressed from the earlier comment. The time-period cited in this instance was a typo. For the ice front loss assumptions, we are applying the closest measured ice dH/dt rate we have to the loss area (reviewer agrees with this) and then assuming that on average the ice was lost mid-way through our period of observations (generally, using a single image pair). This is to avoid the complexity of

determining and handling partial retreats occurring sequentially for a glacier over the study period. We note that the overall impact of the grounded-ice retreats is a small part of the signal we measure.

P3242 line6 change text to 'individual glacier basins' (basins, plural)

Done

P3243 line3 address statement on variation in timing of dDEM and ICESat observations in Table 1

Done, we have improved the description of the timing of the various measurements within the text.

P3244 line6 and line16 word edits Done.

P3244 line25 question on whether we observed, or inferred, kinematic wave propagation

The statement includes citations for two earlier papers and our work here. Taken together, the kinematic wave propagation is 'observed'. However, 'we observe' is an issue since the authorship of the earlier works is not the same as this paper. We adjusted the wording to reflect this better.

P3246 line28 Recognize the difference between mass accumulation and surface mass balance

Changed to 'Surface mass balance (SMB)...

P3258, Fig1 caption: adjust wording for 'climate ice core'. Also, do backgrounds need to be black?

Changed wording to 'ice core'. Re background color, given the variety of colors used, black is the best choice. A blue background would interfere with the color bar colors and the ice shelf extents shown. Grey would be hard to distinguish from the image data. White would be a problem for the basin outlines.

P3259, Fig2 Color changes suggested for ice shelf areas

The ice shelf area color is now grey-blue, and clearly not on the color bar.

P3259, Fig2 and elsewhere: dh/dt or dH/dt?

It is not systematic, it is a function of the span of time spent in compiling the paper and the figures. Since our measurement is of the change in surface height, and not ice thickness, I think the proper convention is: dH/dt . We have converted to this throughout now.

P3256 Table 1 comments

Errors in area determination for ice front retreats are not included specifically in the overall error budget. However, such errors would be far below the cited error. Elevation band for the ice front retreat area is from the first 50 m elevation bin above the lost ice, for all sites. Changed text in footnote c. Footnote h: this is a note

to facilitate the readers understanding of how we determined the column values. The reference text is near the citation of Table 1. The additional footnotes actually save space and are more precise than a text description. I believe most readers would feel that Figures 1 and 2 are complex enough.

SOM comments

Page 2: We have replaced the footnote indicator (footnote was missing) with the URL for the SPIRIT archive.

Table S2 comment We did not undertake this very time-consuming suggestion. Most readers are interested in the mass balance, and we have placed that in the left column near the basin name.

Table S3 comment Short-term variations in mass balance (e.g., when fewer years are averaged) could lead to patterns in the imbalance ratio that do not really indicate long-term glacier 'health'. Granted, in this region everything is changing (SMB, ice flow speed, and elevation) but we believe that the long-term mean mass input is the best one to compare to for an imbalance ratio.

Figure S2 (now S3) caption: Done, added clearer axis labels and standardized on "dH/dt".

1 Review response version submitted to The Cryosphere Discussions, 06 October 2014;
2 Contact: T. Scambos, teds@nsidc.edu, 303/492-1113

3
4
5
6 **Detailed ice loss pattern in the northern Antarctic Peninsula:**
7 **widespread decline driven by ice front retreats**

8
9
10 Ted A. Scambos¹, Etienne Berthier², Terry Haran¹, Christopher A. Shuman³, Alison J.
11 Cook⁴, Stefan R. M. Ligtenberg⁵, and Jennifer Bohlander¹

12
13 ¹National Snow and Ice Data Center (NSIDC), University of Colorado at Boulder, Boulder CO
14 80303 USA

15 ²Laboratoire d'Etudes en Géophysique et Océanographie Spatiales, Centre National de la
16 Recherche Scientifique (LEGOS CNRS), Université de Toulouse, Toulouse 31400 France

17 ³University of Maryland, Baltimore County, Joint Center for Earth Technology (UMBC JCET)
18 at NASA Goddard Space Flight Center, Greenbelt, MD 20771 USA

19 ⁴Department of Geography, Swansea University, Swansea SA2 8PP UK

20 ⁵Institute for Marine and Atmospheric Research Utrecht (IMAU), Utrecht 3508 TA
21 Netherlands

22
23
24 Corresponding author: T.A. Scambos (National Snow and Ice Data Center, University of
25 Colorado, Boulder, 1540 30th Street Bldg. RL-2, Boulder CO 80303, teds@nsidc.edu, +1-
26 303-492-1113).

27
28

29 **Abstract**

30 The northern Antarctic Peninsula (nAP, <66°S) is one of the most rapidly changing
31 glaciated regions on Earth, yet the spatial patterns of its ice mass loss at the glacier
32 basin scale have to date been poorly documented. We use satellite laser altimetry
33 and satellite stereo-image topography spanning 2001-2010, but primarily 2003-
34 2008, to map ice elevation change and infer mass changes for 33 glacier basins
35 covering the mainland and most large islands in the nAP. Rates of ice volume and ice
36 mass change are $27.7 \pm 8.6 \text{ km}^3 \text{ a}^{-1}$ and $24.9 \pm 7.8 \text{ Gt a}^{-1}$. Mass loss is highest for
37 eastern glaciers affected by major ice shelf collapses in 1995 and 2002, where
38 twelve glaciers account for 60% of the total imbalance. However, losses at smaller
39 rates occur throughout the nAP, at both high and low elevation, despite increased
40 snow accumulation along the western coast and ridge crest. We interpret the
41 widespread mass loss to be driven by decades of ice front retreats on both sides of
42 the nAP, and extended throughout the ice sheet due to the propagation of kinematic
43 waves triggered at the fronts into the interior.

44 (184 words)

45
46 **Index terms:**

47 Ice Shelves; Glaciers; Mass Balance; Remote Sensing; Instruments and techniques

48 **Keywords:**

49 Antarctic Peninsula; ICESat; DEM differencing; Larsen B; Larsen A; Prince Gustav
50
51

52 **1 Introduction**

53 The nAP is one of two areas of the Antarctic Ice Sheet showing major mass loss, the
54 other being the Amundsen Sea coast of West Antarctica's ice sheet. Previous studies
55 have shown large negative mass imbalances and significant elevation losses for the
56 nAP (*Ivins et al.*, 2011; *Shepherd et al.*, 2012; *Luthcke et al.*, 2013; *Sasgen et al.*, 2013;
57 *McMillan et al.*, 2014). However, in general these studies have not resolved the
58 spatial distribution of mass imbalance in detail, nor attempted to link patterns of ice
59 loss to processes responsible for the loss. Studies based on gravitational change
60 detection using the Gravity Recovery and Climate Experiment satellite system
61 (GRACE) have an inherent spatial resolution of roughly 250 km scale (*Ivins et al.*,

2011; *Luthcke et al.*, 2013; *Sasgen et al.*, 2013), far larger than the scale of the nAP individual glacier basins and islands. Past altimetry-based studies (*Pritchard et al.*, 2009; *Flament and Rémy*, 2012; *Shepherd et al.*, 2012; *McMillan et al.*, 2014) suffer from either sparse coverage or slope correction issues, or both, due to the steep terrain in the nAP. In the published assessments based on laser altimetry (*Shepherd et al.*, 2012), broad assumptions and large extrapolations are required to interpolate the data across the dissected and rugged Peninsula region. Mass budget methods (*Rignot et al.*, 2004, 2008; *Rott et al.*, 2011; *Shepherd et al.*, 2012), which aim to difference outflowing ice flux and surface mass balance (SMB) for each glacier basin have to date shown results that are difficult to reconcile with other studies of the same glaciers (*Shuman et al.*, 2011; *Berthier et al.*, 2012). This is primarily due to spatially coarse SMB estimates from models or field measurements, difficulties in estimating the cross-sectional area of the glaciers, and differences in the span of time used to estimate ice flux changes (*Berthier et al.*, 2012).

The goal of this study is to determine the spatial pattern of ice elevation changes in the nAP, improve estimates of mass balance for the region, and study the relationship of mass balance with ice shelf collapse and ice front retreats in the area. In light of known climate-related changes in the region, such as increasing surface air temperatures and surface melting, regional sea ice decline, and increasing accumulation (e.g., *Mulvaney et al.* 2012; *Zagorodnov et al.*, 2012; *Stammerjohn et al.*, 2008; *Lenaerts et al.*, 2012; *Barrand et al.*, 2013), our study reveals a pattern of ice mass loss in space and (we infer) in time that may be similar to the characteristics of mass loss in other areas of Antarctica in the coming century.

2 Methods

Our study combines satellite stereo-image digital elevation model differencing (dDEM) with repeat-track laser altimetry from the Ice, Cloud and land Elevation Satellite (ICESat; *Schutz et al.*, 2005), with the objective of providing an assessment of surface elevation change resolved at the scale of the major glacier catchments. We use stereo-image data from the Advanced Spaceborne Thermal Emission and

93 Reflection Radiometer (ASTER; *Fujisada et al.*, 2005) and Satellite Pour
94 l'Observation de la Terre 5 (SPOT5; *Korona et al.*, 2009). Eight satellite stereo-image
95 data sets from the ASTER sensor, and six from the SPOT-5 Haute Résolution
96 Stéréoscopique (HRS) sensor (Table S1 and Figure S1) were processed using
97 previously published methods (*Shuman et al.*, 2011; *Berthier et al.*, 2012; *Gardelle et*
98 *al.*, 2013).

99

100 For the ICESat repeat-track data (Release 633), we used 26 ground tracks from the
101 91-day-repeat orbit crossing the nAP and major ice-covered islands for the high-
102 energy laser campaigns (ICESat Laser 2A through Laser 3J, September 2003 – March
103 2008; *Shuman et al.*, 2006; *Zwally et al.*, 2012). Cross-track elevation adjustment and
104 along-track filtering are used to improve measurement quality, based on surface
105 slopes (not elevations) derived from a recent Antarctic Peninsula DEM (*Cook et al.*,
106 2012). We first eliminated ICESat profile tracks more than 300 meters from the
107 reference track position, and sections where the absolute slope from the gridded
108 DEM was $> \pm 10\%$ slope (or $\pm 5.7^\circ$) for the reference track or measurement track
109 location, or areas where the absolute difference between along-track slopes of the
110 measurement track and reference track exceeded 5% (or $\pm 2.86^\circ$). We further
111 required the ICESat elevation data to be within 50 m (vertically) of the
112 corresponding interpolated DEM elevation. All elevations are referenced to the
113 EGM96 geoid datum. To migrate the measurement track data to the reference track
114 and compare elevations, we identified reference track 'stations' every 43.75 m along
115 the reference track (one-fourth the distance between ICESat altimetry shot locations
116 along track). We then applied an elevation correction based on the difference
117 between the interpolated gridded DEM elevation at the nearest reference track
118 station and the ICESat track data point. ICESat campaign data were compared by
119 differencing their migrated elevations, divided by the time in years between dates of
120 track acquisition. To reduce effects of possible seasonal variations in elevation, we
121 compared only near-integer-year separated repeat profiles, e.g., data from
122 campaigns 2A to 3A (~October, ~1 year apart) or 3B to 3H (~March, ~2 years
123 apart).

124

125 To evaluate different processes in elevation and ice mass change, we treat regions
126 above and below 1000 m above sea level (a.s.l.) separately for each of 33 drainage
127 basins. This is the approximate elevation of an extensive escarpment in the nAP
128 separating plateau areas from individual glacier cirques. Above 1000 m a.s.l., and for
129 islands without sufficient dDEM coverage (Robertson Is., Snow Hill Is., and Joinville,
130 Dundee, and D'Urville islands; Figure 1), the rate of elevation change (dH/dt) is
131 determined from satellite laser altimetry alone. In smooth high elevation areas,
132 correlation of satellite stereo-images often fails due to a lack of high-contrast
133 surface features of sufficient horizontal scale (tens of meters). Below 1000 m a.s.l., a
134 hypsometric interpolation method was applied to individual glacier basins to extend
135 dDEMs and ICESat dH/dt measurements to areas not directly measured. ICESat
136 dH/dt was weighted 10-fold relative to dDEM dH/dt to prevent small dDEM data
137 areas from dominating the weighted dH/dt mapping, and to better utilize the higher
138 accuracy of individual ICESat-based measurements. We used the relationship

139

$$140 \quad dH/dt_{\text{hyps}} = (dH/dt_{\text{DEM}} * (N_{\text{DEM}}/e_{\text{DEM}}) + dH/dt_{\text{ICESat}} * (N_{\text{ICESat}}/e_{\text{ICESat}})) / ((N_{\text{DEM}}/e_{\text{DEM}}) + (N_{\text{ICESat}}/e_{\text{ICESat}})) \quad (1)$$

141

142 where N is the number of measurements within an elevation band (i.e., the number
143 of 50 m grid cells for the dDEMs; or reference track site locations at 43.75 m spacing
144 for ICESat) and e is an inverse weighting of the measurement methods. For dDEMs
145 we used a weight of 1, and for ICESat, we used 0.1. This allowed the fewer but more
146 accurate ICESat-based measurements to contribute to the final result in basins with
147 extensive dDEM coverage. In several areas, ICESat data were available in regions not
148 well covered by dDEM results (see Figure S2).

149

150 We also estimate the above-flotation mass loss of grounded-ice areas that retreated
151 at least 2 km² during the study interval (2001-2010), as identified by image
152 mapping (Cook *et al.*, 2005; Cook and Vaughan, 2010). To estimate the volume and
153 mass loss represented by these areas we mapped the area of retreat during our
154 study period (2001-2010) and half the mean elevation loss rate observed just above

155 the area of grounded ice retreat. This represents an assumption that the vertical
156 elevation change rate of the retreated ice was identical to the region just upstream
157 of the loss area, and that the time of ice front retreat (e.g., when the ice calved and
158 drifted away) was midway through the study period.

159

160 Errors for our assessment of dH/dt (Tables 1 and S2), are based on past analysis of
161 the dDEM method (*Shuman et al., 2011; Berthier et al., 2012*), on inter-comparisons
162 of the two methods at sites having both dDEM and ICESat measurements, and on
163 crossover analysis of ICESat cross-track-corrected data (Table S4). Past analysis for
164 this region suggests that dDEM methods using mixed ASTER and SPOT5 imagery
165 can have a ± 5 m uncertainty for individual glacier basins, i.e. ~ 1 m a^{-1} given a 5-yr
166 time separation between DEMs. However, examining our ICESat and dDEM dH/dt at
167 sites with both measurements (6158 sites) shows that the methods differ by just
168 ~ 0.3 m a^{-1} overall, a difference that ranges between 0.07 to 0.75 m a^{-1} over various
169 sub-sets of our measurements (Table S4). This is in agreement with our previous
170 study that showed reduced errors when dDEM results are averaged over basin-scale
171 areas (*Berthier et al., 2012*). Seven crossover sites with slope-corrected ICESat
172 dH/dt measurements show good agreement with the dDEM measurements at the
173 same locations (mean offset of $+0.05$ m a^{-1}).

174

175 Errors in the ICESat cross-track correction for dH/dt are more dependent on slope
176 errors in the Cook et al. (2012) DEM and not its absolute elevation accuracy.
177 Assuming our selection criteria eliminated regions of significant error in the DEM,
178 we estimate that across-track or along-track slopes in the Cook et al. (2012) DEM
179 are accurate to within $\pm 0.5^\circ$ over a length scale of 300 m, or ± 8.7 m km^{-1} . A test of
180 this was conducted by comparing the Cook et al. (2012) DEM slopes with a DEM
181 acquired in 2009 by the NASA Land, Vegetation, and Ice Sensor (LVIS) airborne laser
182 altimeter, covering about 20% of the study region. This showed that the mean
183 difference in along-track slope in the overlap region was $0.06 \pm 1.2^\circ$ when our
184 criteria are applied to both data sets. For laser altimetry measurements alone, our
185 inferred mean slope error of $\pm 0.5^\circ$ implies a mean laser measurement pair cross-

186 track correction error of ± 1.31 m (assuming a mean cross-track distance of 150 m).
187 We assume this error is randomly distributed when averaging over a glacier basin.
188 Thus for the average of 20 measurement sites, the mean error is <25 cm. Since laser
189 measurement pairs may have 1 to 4 years separation in time, and many have
190 multiple measurements at a single site (see Figure S2), our overall mean error in
191 elevation change rate is significantly less than this. Additionally, the majority of the
192 basins we consider have many more than 20 measurement sites (Table S2).

193
194 Considering all sources of error, and variations in the time-span of measurements
195 for dDEM and ICESat measurements, data density variations for the basins, and the
196 strong agreement between these independent altimetric methods, we adopt a mean
197 error of ± 0.15 m a^{-1} for regions of laser altimetry measurement alone (above 1000
198 m a.s.l.), and ± 0.3 m a^{-1} for our dDEM plus altimetry measurements (below 1000 m
199 a.s.l.) and the glacier basins, islands, and sub-basins without laser altimetry. Errors
200 for volume and mass change determinations thus scale with area.

201

202 **3 Results**

203 An overview of our results is shown in Figure 2 and Table 1, and detailed basin-by-
204 basin values are provided in supplementary Table S2. The results show that basins
205 impacted by recent ice shelf loss and ice front retreat have very high rates of change,
206 but also indicate that few areas — high or low, east or west — have positive dH/dt .
207 Recent ice-shelf loss (ISL) basins (losses since 1986, and particularly in 1995 and
208 2002), all on the eastern side of the nAP, and four smaller glaciers with recent
209 grounded ice front loss (IFL; losses since 2000) on the western and northeastern side
210 of the nAP, show a characteristic pattern of very high elevation loss rates just
211 upstream of the ice front but far lower elevation loss rates at high elevation. Mean
212 elevation change for areas below 1000 m a.s.l. at 12 eastern-side ISL glacier basins
213 (or sub-basins) is -2.6 m a^{-1} (range, $+0.4$ to -5.8 m a^{-1}) and -2.2 m a^{-1} (-2.0 to -2.7 m a^{-1})
214 for the four western-side and northeastern IFL sub-basins experiencing recent ice
215 front retreat (>2 km² since 2000). At elevations >1000 m, elevation loss in the
216 eastern ISL basins is small (mean, -0.10 m a^{-1} ; range $+0.35$ to -0.54 m a^{-1}). Glacier

217 systems on the western nAP coast and the western islands below 1000 m a.s.l.,
218 excluding the recent IFL regions, are changing at various rates (typically $\sim -0.15 \text{ m a}^{-1}$,
219 range $+0.7$ to -1.6 m a^{-1}). However, western-side basins are losing elevation at
220 significant rates above 1000 m a.s.l. (mean of -0.59 m a^{-1} ; range -0.25 to -1.30 m a^{-1}).

221

222 We examine the rates of surface elevation change and cumulative ice volume change
223 as they vary with altitude for three sub-regions of the study area in Figure 3. The
224 patterns of elevation change with altitude illustrate the differences between the
225 western-side glacier and island regions and the eastern-side ISL areas, and also
226 highlight the bi-modal hypsometry pattern characteristic of the nAP. Eastern-side
227 ISL areas show dramatically decreasing elevation with time, large volume changes
228 at low elevations, and little or no significant change in the upper-most catchment
229 areas (Figure 3c-d). Western-side glaciers show mildly negative rates of elevation
230 change at all elevations, and a steady cumulative volume decrease rate with altitude.
231 The major glaciers of Scar Inlet Ice Shelf, the lone remaining large ($>50 \text{ km}^2$) ice
232 shelf in the study area with significant tributary glaciers, show a unique pattern of
233 ice losses at low elevation and some areas of thickening at altitude. We believe this
234 is likely the pattern of elevation change present for the eastern nAP ISL glacier
235 systems in the years immediately prior to shelf disintegration.

236

237 **4 Discussion**

238 The widespread elevation losses suggested here for both sides of the nAP at high
239 elevations, and especially for the western side of the divide, have significant
240 implications for the region's recent mass change history. Moreover, the detailed
241 mapping on a basin-by-basin scale supports model and GPS studies of local bedrock
242 uplift. A recent study (*Neild et al., 2014*), using an earlier (near-final) version of our
243 presented data combined with continuous GPS uplift measurements at sites in the
244 Peninsula, modelled both the elastic response and long-term isostatic rebound in
245 the region, showing that the nAP is underlain by very low viscosity mantle. They
246 further conclude that there is little or no continuing uplift (observed or modelled) as
247 a result of mass loss during the Last Glacial Maximum (LGM). The results are

248 supported by the general conclusions of papers discussing the post-LGM evolution
249 of the eastern Peninsula (*Domack et al., 2005; Rebesco et al., 2014*) which state that
250 the majority of ice sheet retreat occurred by about 12,000 years ago. If so, mantle
251 rebound from those events would be complete at this point.

252

253 Previous observational studies have shown that the elevation decline pattern for ISL
254 or IFL glaciers migrates upstream and diffuses on a scale of years to decades (*Howat*
255 *et al., 2007; Joughin et al., 2008; Shuman et al., 2011; Berthier et al., 2012*),
256 consistent with kinematic wave models of glacier response to ice front stress
257 changes for tidewater glaciers (*Pfeffer, 2007; Nick et al., 2009; Favier et al., 2014*). In
258 past work in this area (*Shuman et al., 2011; Berthier et al., 2012*), and with
259 comparison to these results, we observe that eastern ISL glaciers are currently
260 propagating kinematic waves upstream from their lower trunk areas, but this
261 process has not yet had a significant impact on higher elevations. Western-coast
262 nAP glacier front retreats, elevation losses, and accelerations have been
263 documented (*Cook and Vaughan, 2005; Pritchard and Vaughan, 2007; Kunz et al.,*
264 *2012*), with a major pulse of retreat beginning in the 1970s. Moreover, our work
265 here shows that on-going ice front losses within the study period behave much like
266 smaller versions of the eastern-side glaciers impacted by ice shelf and glacier front
267 retreat (Table 1). The earlier losses inferred for the western side fjord glaciers (e.g.,
268 *Christ et al., 2014*) appear to have now propagated throughout the entirety of the
269 western basins, leading to significant and widespread surface lowering in the
270 western upper catchment areas (>1000 a.s.l.) at greater rates than for the eastern
271 side on average (Table 1 and Table S2).

272

273 However, any measurement of elevation or mass losses along the western coast and
274 in the upper elevation areas must be reconciled with a large recent positive mass
275 accumulation anomaly. Ice cores at two sites on the nAP ridge crest (Detroit Plateau,
276 64.08°S, 59.65°W, 1937 m a.s.l., and Site Beta of the Larsen Ice Shelf System,
277 Antarctica, 66.03°S, 64.04°W, 1980 m a.s.l.; Figure 1) show significant increases in
278 accumulation in the late 20th century: 2052 to 2776 kg m² a⁻¹ from 1981-87 to 2001-

279 07, and 1750 to 2710 kg m² a⁻¹ from 1960-69 to 2000-08, respectively (*Potocki et al.*,
280 2011; *Goodwin*, 2013). Models of precipitation input for the region (*Saha et al.*,
281 2010; *Dee et al.*, 2011; *Lenaerts et al.*, 2012) also show a strong overall increase for
282 the most recent decades, but some indicate a slight decline in the last decade,
283 covering our dH/dt measurement period (*Saha et al.*, 2010; *Lenaerts et al.*, 2012;
284 *Shepherd et al.*, 2012). The large increase and later reduction in accumulation are
285 associated with multi-decadal warming (*Barrand et al.*, 2013) and associated
286 reductions in sea ice extent northwest of the nAP (*Stammerjohn et al.*, 2012)
287 recently moderated by a slight cooling trend (*Blunden and Arndt*, 2012; *Zagorodnov*
288 *et al.*, 2012).

289

290 Multi-decadal accumulation, temperature and snowmelt trends cause changes in the
291 compaction rate of snow and firn, and can potentially impact measurements of
292 surface elevation change (*Ligtenberg et al.*, 2011). Using a model climate time series
293 (based on reanalysis of weather data) spanning the period of our measurements
294 (RACMO-2.1/ANT; *Lenaerts et al.*, 2012), a dH/dt for the firn column at 27 km
295 spatial scale is obtained similar to that used in previous related analyses (*Pritchard*
296 *et al.*, 2012; *Gardner et al.*, 2013). The modelled inter-annual variability in
297 accumulation, temperature and snowmelt, and their effect on firn compaction result
298 in dH/dt corrections between -0.19 to +0.12 m a⁻¹ on the grounded ice of the nAP,
299 with generally positive (thickening) corrections on the western side and negative to
300 the east. The small effect on the firn layer, and the high variability of accumulation
301 both inter-annually and among the basin areas (Figure 4a) make the correction
302 relatively insignificant. We therefore report dH/dt as observed from the satellite
303 data. From these observations, we report mass change in Table 1 and Table S2 as:

304

$$305 \quad (dH/dt)_{\text{hyps}} * (A) * \rho \quad (2)$$

306

307 where $(dH/dt)_{\text{hyps}}$ is the elevation-band-weighted mean measured dH/dt, A is area
308 of the glacier basin or island, and ρ is our assumed mean density of ice and firn lost
309 by dynamics (900 kg m⁻³). We eliminated the nunatak areas from each of the basins,

310 based on the Antarctic Digital Database mapping of rock outcroppings in the region
311 similar to previous studies (e.g., *Gardner et al.*, 2013).

312

313 Our estimate of mass balance for the combined nAP region is $-24.9 \pm 7.8 \text{ Gt a}^{-1}$, with
314 the great majority of the mass loss occurring at elevations below 1000 m a.s.l. ($-$
315 $21.9 \pm 6.3 \text{ Gt a}^{-1}$, or 88%; Table 1). Regionally, the eastern nAP basins dominate the
316 mass loss at $-17.7 \pm 3.7 \text{ Gt a}^{-1}$, or 72% of the loss, and of this, $-15.2 \pm 3.2 \text{ Gt a}^{-1}$ (60%) is
317 from 12 glacier basins flowing into embayments formerly occupied by the Prince
318 Gustav, Larsen Inlet, Larsen A, and Larsen B ice shelves. For the 11 western nAP
319 glacier basins and islands, the mass loss rate is similar at low and high elevations ($-$
320 $2.3 \pm 0.7 \text{ Gt a}^{-1}$ $>1000 \text{ m a.s.l.}$, and $-2.2 \pm 1.0 \text{ Gt a}^{-1}$ below). Overall, the nAP region
321 accounts for $\sim 29\%$ of Antarctica mass imbalance during the study period (*Shepherd*
322 *et al.*, 2012).

323

324 We also examined the mass balance ratio of the basins and regional areas, based on
325 mass input, primarily snow accumulation (*Lenaerts et al.*, 2012; Table 2, Table S3).
326 Surface mass balance (SMB) in the region has a very large gradient from west to
327 east, with values of $1500 \text{ to } 3000 \text{ kg m}^{-2} \text{ a}^{-1}$ for the western areas and high
328 elevations dropping to $\sim 500 \text{ to } 1500 \text{ kg m}^{-2} \text{ a}^{-1}$ in the low elevation areas of the
329 eastern nAP coast. A ratio of the mass balance divided by the mass accumulation
330 input indicates the degree of imbalance in the glacier systems, and suggests the level
331 of ice flux increase for glacier systems having recently accelerated due to ice front or
332 ice shelf losses. We term this value the imbalance ratio. The imbalance ratio for the
333 nAP as a whole is -0.45 , implying that mass outflow is 45% greater during the study
334 period relative to a steady-state rate in the current climate. For the eastern nAP
335 glaciers, the ratio is $-0.3 \text{ to } -3.2$ (average, -0.8) with the major ISL glaciers in the
336 Larsen A and Larsen B between $-0.33 \text{ and } -3.4$. The upper areas of these glacier
337 systems are essentially balanced (~ -0.1). IFL glaciers along the western and
338 northern coastlines have imbalance ratios similar to the ISL glaciers, $\sim -0.5 \text{ to } -2.4$.

339

340 Our mass balance estimate for the nAP region agrees well with recently published

341 gravimetric values, although in some cases we believe this is coincidental. Recent
342 GRACE-based estimates that can be most easily compared with our study yield
343 values of $-27.5 \pm 10 \text{ Gt a}^{-1}$ (summing the mascons encompassing and adjacent to our
344 study area) (*Luthcke et al., 2013*), and $26 \pm 3 \text{ Gt a}^{-1}$ for a larger GRACE mascon
345 extending to 70°S (*Sasgen et al., 2013*). Due to the low spatial resolution of the
346 gravimetric measurement, both these GRACE-derived results inherently include
347 portions of the Larsen C Ice Shelf and adjacent ice-covered islands we did not
348 measure (notably, King George Island) that lost elevation and mass during the
349 ICESat period (*Gardner et al., 2013*). Similarly, the strong east-west gradient
350 revealed in our study is not discernable by the GRACE system. Overall, however, the
351 GRACE results provide a good summary confirmation for our study, and imply that
352 nearly all of the mass loss for the Peninsula lies in, the nAP region defined here.

353

354 For earlier ICESat-only studies of the mass balance in the area (*Shepherd et al.,*
355 *2012*), the apparent agreement is likely fortuitous. Simple extrapolation methods
356 that do not include information about individual basin dynamics (e.g.,
357 spatial/elevation extent, ice shelf loss, east-west variations), lead to very different
358 values for total mass change. We conducted two experiments using our cross-track
359 adjusted ICESat data alone to examine the scale of possible discrepancies. With an
360 assumption of uniform mean elevation change for each elevation band throughout
361 the nAP, the volume change from ICESat data would be $-36.6 \text{ km}^3 \text{ a}^{-1}$. This
362 overestimate derives from ISL glaciers forming too great a part of the net elevation
363 change measurement data, especially for their lower elevations. This is, in part, due
364 to more ICESat data being acquired along the eastern nAP, likely a result of less
365 cloud cover there. If one partially addresses this by separating ICESat data in two
366 subsets (ISL basins vs the rest), the volume change is still 10% greater than our
367 study, $-30.6 \text{ km}^3 \text{ a}^{-1}$.

368

369 The most recent assessment of the mass balance of the entire Peninsula uses
370 CryoSat-2 interferometric radar altimetry data to infer a mass balance of $-23 \pm 18 \text{ Gt}$
371 a^{-1} for a period following our evaluation, 2010-2013 (*McMillan et al., 2014*). The

372 agreement is well within both studies' error bars, and suggests that mass imbalance
373 for the Peninsula is not changing significantly at the present time. However, a more
374 detailed study of a set of glacier outlets that formerly fed the Larsen A and Prince
375 Gustav ice shelves suggests that this area (which was the site of major ice shelf
376 disintegrations in 1988 and 1995) has begun to see a slightly reduced level of ice
377 mass loss in the 2011-2013 period (H. Rott, pers. comm., 2014).

378

379 We now examine the potential impact of further ice shelf loss in the Scar Inlet
380 region, a remnant ice shelf section from the Larsen B Ice Shelf. Comparing high-
381 resolution bathymetric mapping of the seabed exposed by nAP-wide ice shelf loss
382 and glacier retreat with our data in Figure 1 shows that it is the glaciers with deep
383 (>500 m) troughs and recent ice shelf loss that have the greatest elevation loss and
384 mass imbalance (*Zgur et al., 2007; Shuman et al., 2011; Rebesco et al., 2014*). Recent
385 ice-thickness maps of the tributary glaciers (Starbuck, Flask, and Leppard glaciers)
386 of the still-intact Scar Inlet Ice Shelf (SIIS) indicate they have unusually deep glacier
387 troughs just behind the grounding line, well in excess of 1000 m below sea level in
388 the case of Flask Glacier, and 500 m below sea level for Starbuck glacier (*Farinotti et*
389 *al., 2013, Farinotti et al., 2014*). From Table S3, the mean imbalance ratio of ISL
390 glaciers with ice-front bathymetric troughs exceeding 500 m depth is -1.20, and -
391 3.18 for those exceeding 1000 m depth. (for comparison, it is +0.07 for trough areas
392 less than 500 m depth). If we assume that the three primary tributary glaciers of SIIS
393 will experience the same mean imbalance ratio following a collapse of their frontal
394 ice shelf in Scar Inlet, we can anticipate increased mass imbalance in those basins,
395 from the -1.36 Gt a⁻¹ observed during our study period to ~-5.5 Gt a⁻¹.

396

397 **5 Conclusions**

398 Overall, our study suggests that the nAP mass imbalance pattern is a combination of
399 several recent changes to the coastal glaciers and ice shelf systems, likely beginning
400 several decades ago along the western coastal fjords and islands, with extensive
401 inland propagation of mass loss to the ice divide area, and more recent ice shelf loss
402 along the eastern flanks and islands with extensive and expanding inland

403 propagation. Further, the large measured increase in snow accumulation over the
404 past few decades has not created vast regions of positive mass balance suggesting
405 that negative mass balances will continue into the future.

406

407 **Authorship contributions**

408 *T. Scambos led the writing and compilation of graphics and tables, and with T. Haran and J.*
409 *Bohlander, conducted the ICESat-based elevation change analysis. E. Berthier conducted the*
410 *differential DEM analysis and integrated the ICESat data with the dDEM data. C. Shuman and*
411 *A. Cook evaluated glacier front area changes and C. Shuman produced components of Figure 4.*
412 *A. Cook provided the glacier basin outlines. S. Ligtenberg evaluated the firn compaction and*
413 *accumulation variability estimates, and their impact on our results. All co-authors contributed*
414 *to the writing of the paper.*

415

416 **Acknowledgements**

417 The ICESat data for this paper are available at the NASA Distributed Active Archive
418 Center at NSIDC (GLA12 - GLAS/ICESat L2 Antarctic and Greenland Ice Sheet
419 Altimetry Data). The SPOT5 HRS data were provided at no cost by CNES through the
420 SPIRIT project. The ASTER data were provided at no cost by NASA/USGS through
421 the Global Land Ice Measurements from Space (GLIMS) project. This work was
422 supported by NASA grant NNX10AR76G to T. Scambos and W. Abdalati, the TOSCA
423 and ISIS programs of the French Space Agency (CNES) to E. Berthier, NASA
424 Cryospheric Program funds to C. Shuman, NSF grant ANT-0732921 to T. Scambos,
425 and the Netherlands Polar Program and European Union Seventh Framework
426 Programme grant 226375 to S. Ligtenberg.

427

428

429 **References**

430

431 Barrand, N. E., Vaughan, D. G., Steiner, N., Tedesco, M., Kuipers Munneke, P., van den
432 Broeke, M. J., and Hosking, J. S.: Trends in Antarctic Peninsula surface melting
433 conditions from observations and regional climate modeling, *J. Geophys Res.*,
434 118(1), 315–330, doi:10.1029/2012JF002559, 2013.

- 435 Berthier, E., Scambos, T. A., and Shuman, C. A.: Mass loss of Larsen B tributary
436 glaciers (Antarctic Peninsula) unabated since 2002, *Geophys. Res. Lett.*, 39
437 L13501, doi:10.1029/2012GL051755, 2012.
- 438 Blunden, J., and Arndt, D. S.: State of the Climate in 2011, *Bull. Amer. Meteor. Soc.*,
439 93(7), S1–S282, doi:10.1175/2012BAMSStateoftheClimate.1., 2012.
- 440 Christ, A., Talia-Murray, M., Elking, N., Domack, E., Leventer, A., Lavoie, C., Brachfield,
441 S., Yoo, K.-C., Gilbert, R., Jeong, S.-M., Petrushak, S., Wellner, J.: Late Holocene
442 glacial advance and ice shelf growth in Barilari 1 Bay, Graham Land, west
443 Antarctic Peninsula, *Geol. Soc. Am. Bull.*, doi:10.1130/B31035, 2014.
- 444 Cook, A. J., and Vaughan, D. G.: Overview of areal changes of the ice shelves on the
445 Antarctic Peninsula over the past 50 years, *The Cryosphere*, 4(1), 77–98,
446 doi:10.5194/tc-4-77-2010, 2010.
- 447 Cook, A. J., Fox, A. J., Vaughan, D. G., and Ferrigno, J. G.: Retreating glacier fronts on
448 the Antarctic Peninsula over the past half-century, *Science*, 308(5721), 541–
449 544, 2005.
- 450 Cook, A. J., Murray, T., Luckman, A., Vaughan, D. G., and Barrand, N. E.: A new 100-m
451 Digital Elevation Model of the Antarctic Peninsula derived from ASTER
452 Global DEM: methods and accuracy assessment, *Earth System Science Data*,
453 4, 129–142, doi:10.5194/essd-4-129-2012, 2012.
- 454 Dee, D. P., Uppala, S. M., Simmons, A. J., Berrisford, P., Poli, P., Kobayashi, S., Andrae,
455 U., Balmaseda, M. A., Balsamo, G., Bauer, P., Bechtold, P., Beljaars, A. C. M., van
456 de Berg, L., Bidlot, J., Bormann, N., Delsol, C., Dragani, R., Fuentes, M., Geer, A.
457 J., Haimberger, L., Healy, S. B., Hersbach, H., Hólm, E. V., Isaksen, I., Kållberg,
458 P., Köhler, M., Matricardi, M., McNally, A. P., Monge-Sanz, B. M., Morcrette, J.-J.,
459 Park, B.-K., Peubey, C., de Rosnay, P., Tavolato, C., Thépaut, J.-N. and Vitart, F.:
460 The ERA-Interim reanalysis: configuration and performance of the data
461 assimilation system, *Q. Jour. Royal Met. Soc.*, 137(656), 553–597,
462 doi:10.1002/qj.828, 2011.
- 463 Domack, E., Duran, D., Leventer, A., Ishman, S., Doane, S., McCallum, S., Abblas, D.,
464 Ring, J., Gilbert, R., and Prentice, M.: Stability of the Larsen B ice shelf on the
465 Antarctic Peninsula during the Holocene epoch, *Nature*, 436(7051), doi:
466 10.1038/nature03908, 681–685.
- 467 Farinotti, D., Corr, H., and Gudmundsson, G. H.: The ice thickness distribution of
468 Flask Glacier, Antarctic Peninsula, determined by combining radio-echo
469 soundings, surface velocity data and flow modelling, *Ann. Glaciol.*, 54(63),
470 18–24, doi:10.3189/2013AoG63A603, 2013.
- 471 Farinotti, D., King, E. C., Albrecht, A., Huss, M., and Gudmundsson, G. H.: The bedrock
472 topography of Starbuck Glacier, Antarctic Peninsula, as measured by radio-

- 473 echo sounding, *Ann. Glaciol.*, 55(67), 22–28, doi:10.3189/2014AoG67A025,
474 2014.
- 475 Favier, L., Durand, G., Cornford, S. L., Gudmundsson, G. H., Gagliardini, O., Gillet-
476 Chaulet, F., Zwinger, T., Payne, A. J., and Le Brocq. A. M.: Retreat of Pine Island
477 Glacier controlled by marine ice-sheet instability, *Nature Clim. Change*, 4(2),
478 117–121, doi:10.1038/nclimate2094, 2014
- 479 Flament, T., and Rémy, F: Dynamic thinning of Antarctic glaciers from along-track
480 repeat radar altimetry, *J. Glaciol.*, 58(211), 830–840,
481 doi:10.3189/2012JoG11J118, 2012.
- 482 Fujisada, H., Bailey, G. B., Kelly, G. G., Hara, S., and Abrams, M. J.: ASTER DEM
483 performance, *IEEE T. Geosci. Remote Sens.*, 43(12), 2707–2714, 2005
- 484 Gardelle, J., Berthier, E., Arnaud, Y., and Käab, A.: Region-wide glacier mass balances
485 over the Pamir-Karakoram-Himalaya during 1999–2011, *The Cryosphere*, 7,
486 1263–1286, doi:10.5194/tc-7-1263-2013, 2013.
- 487 Gardner, A. S., Moholdt, G., Cogley, J. G., Wouters, B., Arendt, A. A., Wahr, J., Berthier,
488 E., Hock, R., Pfeffer, W. T., Kaser, G., Ligtenberg, S. R. M., Bolch, T., Sharp, M. J.,
489 Hagen, J. O., van den Broeke, M. R., and Paul, F.: A Reconciled Estimate of
490 Glacier Contributions to Sea Level Rise: 2003 to 2009, *Science*, 340(6134),
491 852–857, doi:10.1126/science.1234532, 2013.
- 492 Goodwin, B. P.: Recent Environmental Changes on the Antarctic Peninsula as
493 Recorded in an ice core from the Bruce Plateau. PhD diss., The Ohio State
494 University, Columbus, OH, 247 pp., 2013.
- 495 Haran, T., Bohlander, J., Scambos, T. and Fahnestock, M.: MODIS Mosaic of Antarctica
496 2004 (MOA2004) Image Map. Boulder, Colorado USA: National Snow and Ice
497 Data Center, doi:10.7265/N5ZK5DM5, 2005, updated 2014.
- 498 Haran, T., Bohlander, J., Scambos, T., Painter, T., and Fahnestock, M.: MODIS Mosaic
499 of Antarctica 2008-2009 (MOA2009) Image Map. Boulder, Colorado USA:
500 National Snow and Ice Data Center, doi:10.7265/N5KP8037, 2014.
- 501 Howat, I. M., Joughin, I., and Scambos, T. A.: Rapid Changes in Ice Discharge from
502 Greenland Outlet Glaciers, *Science*, 315(5818), 1559–1561, 2007.
- 503 Ivins, E. R., Watkins, M. M., Yuan, D.-N., Dietrich, R., Casassa, G., and Rülke, A.: On-
504 land ice loss and glacial isostatic adjustment at the Drake Passage: 2003–
505 2009, *J. Geophys. Res.-Earth*, 116, B02403, doi:10.1029/2010JB007607,
506 2011.
- 507 Joughin, I., Howat, I. M., Fahnestock, M., Smith, B., Krabill, W., Alley, R. B., Stern, H.,
508 and Truffer, M.: Continued evolution of Jakobshavn Isbrae following its rapid

509 speedup, *J. Geophys. Res.-Earth*, 113, F04006, doi:10.1029/2008JF001023,
510 2008.

511 Korona, J., Berthier, E., Bernard, M., Rémy, F., and Thouvenot, E.: SPIRIT. SPOT 5
512 stereoscopic survey of Polar Ice: Reference Images and Topographies during
513 the fourth International Polar Year (2007-2009), *ISPRS J. Photogramm.*, 64,
514 204–212, doi:10.1016/j.isprsjprs.2008.10.005, 2009.

515 Kunz, M., King, M. A., Mills, J. P., Miller, P. E., Fox, A. J., Vaughan, D. G., and Marsh, S.
516 H.: Multi-decadal glacier surface lowering in the Antarctic Peninsula,
517 *Geophys. Res. Lett.*, L19502, 10.1029/2012GL052823, 2012.

518 Lenaerts, J. T. M., van den Broeke, M. R., van de Berg, W. J., van Meijgaard, E., and
519 Munneke, P. K.: A new, high-resolution surface mass balance map of
520 Antarctica (1979-2010) based on regional atmospheric climate modeling,
521 *Geophys. Res. Lett.*, 39, L04501, 4501–4501, doi:10.1029/2011GL050713,
522 2012.

523 Ligtenberg, S. R. M., Helsen, M. M., and van den Broeke, M. R.: An improved semi-
524 empirical model for the densification of Antarctic firn, *The Cryosphere*, 5(4),
525 809–819, doi:10.5194/tc-5-809-2011, 2011.

526 Luthcke, S. B., Sabaka, T. J., Loomis, B. D., Arendt, A. A., McCarthy, J. J., and Camp, J.:
527 Antarctica, Greenland and Gulf of Alaska land-ice evolution from an iterated
528 GRACE global mascon solution, *J. Glaciol.* 59, 613–631,
529 doi:10.3189/2013JoG12J147, 2013.

530 McMillan, M., Shepherd, A., Sundal, A., Briggs, K., Muir, A., Ridout, A., Hogg, A., and
531 Wingham, D.: Increased ice losses from Antarctica detected by CryoSat-2,
532 *Geophys. Res. Lett.* 41, 1-7, doi:10.1002/2014GL060111, 2014.

533 Mulvaney, R., Abram, N. J., Hindmarsh, R. C., Arrowsmith, C., Fleet, L., Triest, J., ... &
534 Foord, S.: Recent Antarctic Peninsula warming relative to Holocene climate
535 and ice-shelf history, *Nature* 489(7414), doi:10.1038/nature11391, 141-
536 144., 2012.

537 Nick, F. M., Vieli, A., Howat, I. M., and Joughin, I.: Large-scale changes in Greenland
538 outlet glacier dynamics triggered at the terminus, *Nature Geosci.*, 2(2), 110–
539 114, 2009.

540 Nield, G. A., Barletta, V. R., Bordoni, A., King, M. A., Whitehouse, P. L., Clarke, P. J.,
541 Domack, E., Scambos, T., and Berthier, E.: Rapid bedrock uplift in the
542 Antarctic Peninsula explained by viscoelastic response to recent ice
543 unloading, *Earth and Planetary Science Letters*, 397, doi:
544 10.1016/j.epsl.2014.04.019, 32-41, 2014.

- 545 Pfeffer, W. T.: A simple mechanism for irreversible tidewater glacier retreat, J.
546 Geophys. Res.-Earth, 112 (F3), F03S25, doi:10.1029/2006JF000590, 2007.
- 547 Potocki, M., Mayewski, P. A., Kurbatov, A., Handley, M., Simoes, J. C., and Jaña, R.:
548 Detailed glaciochemical records from a northern Antarctic Peninsula site-
549 Detroit Plateau. In AGU Fall Meeting Abstracts, 1, p. 1822, 2011, San
550 Francisco, 5-9 December, 2011.
- 551 Pritchard, H. D., and Vaughan, D. G.: Widespread acceleration of tidewater glaciers
552 on the Antarctic Peninsula, J Geophys Res-Earth, 112(F3), F03S29,
553 doi:10.1029/2006JF000597, 2007.
- 554 Pritchard, H. D., Arthern, R. J., Vaughan, D. G., and Edwards, L. A.: Extensive dynamic
555 thinning on the margins of the Greenland and Antarctic ice sheets, Nature,
556 461(7266), 971–975, 2009.
- 557 Pritchard, H. D., Ligtenberg, S. R. M., Fricker, H. A., Vaughan, D. G., van den Broeke, M.
558 R., and Padman, L.: Antarctic ice-sheet loss driven by basal melting of ice
559 shelves, Nature, 484(7395), 502–505, doi:10.1038/nature10968, 2012.
- 560 Rebesco, M., Domack, E., Zgur, F., Leventer, A., Lavoie, C., Brachfeld, S., Willmott, V.,
561 Halverson, G., Truffer, M., Scambos, T., Smith, J., and Pettit, E.: Boundary
562 condition of grounding lines prior to collapse, Larsen-B Ice Shelf, Antarctica.
563 Science 345(6202), doi:10.1126/science.1256697, 2014.
- 564 Rignot, E., Casassa, G., Gogineni, P., Krabill, W., Rivera, A., and Thomas, R.:
565 Accelerated ice discharge from the Antarctic Peninsula following the collapse
566 of Larsen B ice shelf, Geophys. Res. Lett., 31, L18401, 2004.
- 567 Rignot, E., Bamber, J. L., van den Broeke, M. R., Davis, C., Li, Y. H., van de Berg, J., and
568 van Meijgaard, E.: Recent Antarctic ice mass loss from radar interferometry
569 and regional climate modelling, Nat. Geosci., 1(2), 106–110,
570 doi:10.1038/ngeo102, 2008.
- 571 Rott, H., Müller, F., Nagler, T., and Floricioiu, D.: The imbalance of glaciers after
572 disintegration of Larsen B ice shelf, Antarctic Peninsula, The Cryosphere,
573 5(1), 125–134, doi:10.5194/tc-5-125-2011, 2011.
- 574 Saha, S., Moorthi, S., Wu, X., Wang, J., Nadiga, S., Tripp, P., Behringer, D., Hou, Y.-T.,
575 Chuang, H.-Y., Iredell, M., Ek, M., Meng, J., Yang, R., Mendez, M. P., van den
576 Dool, H., Zhang, Q., Wang, W., Chen, M., Becker, E. (2013). The NCEP climate
577 forecast system version 2. Journal of Climate, 27, doi:10.1175/JCLI-D-12-
578 00823.1, 2013.
- 579 Sasgen, I., H. Konrad, E. R. Ivins, M. R. Van den Broeke, J. L. Bamber, Z. Martinec, and
580 V. Klemann (2013), Antarctic ice-mass balance 2003 to 2012: regional
581 reanalysis of GRACE satellite gravimetry measurements with improved

- 582 estimate of glacial-isostatic adjustment based on GPS uplift rates, *The*
583 *Cryosphere*, 7(5), 1499–1512, doi:10.5194/tc-7-1499-2013, 2013.
- 584 Scambos, T. A., Haran, T. M., Fahnestock, M. A., Painter, T. H., and Bohlander, J.:
585 MODIS-based Mosaic of Antarctica (MOA) data sets: Continent-wide surface
586 morphology and snow grain size, *Remt. Sens. Environ.*, 111(2), 242-257,
587 2007.
- 588 Schutz, B. E., Zwally, H. J., Shuman, C. A., Hancock, D., and DiMarzio, J. P. : Overview of
589 the ICESat mission. *Geophys. Res. Lett.*, 32(21), L21S01, doi:
590 10.1029/2005GL024009, 2005.
- 591 Shepherd, A., Ivins, E. R., A, G., V. R., Bentley, M. J., Bettadpur, S., Briggs, K., Bromwich,
592 D. H., Forsberg, R., Galin, N., Horwath, M., Jacobs, S., Joughin, I., King, M. A.,
593 Lenaerts, J. T. M., Li, J., Ligtenberg, S. R. M., Luckman, A., Luthcke, S. B.,
594 McMillan, M., Meister, R., Milne, G., Mouginot, J., Muir, A., Nicolas, J. P., Paden,
595 J., Payne, A. J., Pritchard, H., Rignot, E., Rott, H., Sørensen, L. S., Scambos, T. A.,
596 Scheuchl, B., Schrama, E. J. O., Smith, B., Sundal, A. V., J. H., van de Berg, W. J.,
597 van den Broeke, M. R., Vaughan, D. G., Velicogna, I., Wahr, J., Whitehouse P. L.,
598 Wingham, D. J., Yi, D., Young, D., and Zwally, H. J.: A Reconciled Estimate of
599 Ice-Sheet Mass Balance, *Science*, 338(6111), 1183–1189,
600 doi:10.1126/science.1228102, 2012.
- 601 Shuman, C. A., Zwally, H. J., Schutz, B. E., Brenner, A. C., DiMarzio, J. P., Suchdeo, V. P.,
602 and Fricker, H. A.: ICESat Antarctic elevation data: preliminary precision and
603 accuracy assessment, *Geophys. Res. Lett.* 33(7), L07501, doi:
604 10.1029/2005GL025227, 2007.
- 605 Shuman, C. A., Berthier, E., and Scambos, T. A.: 2001-2009 elevation and mass losses
606 in the Larsen A and B embayments, Antarctic Peninsula, *J. Glaciol.*, 57(204),
607 737–754, doi:10.3189/002214311797409811, 2011.
- 608 Stammerjohn, S. E., D. G. Martinson, R. C. Smith, X. Yuan, and D. Rind, D.: Trends in
609 Antarctic annual sea ice retreat and advance and their relation to El Niño–
610 Southern Oscillation and Southern Annular Mode variability, *J. Geophys. Res.*
611 *Oceans* (1978–2012), 113(C3), C03S90, doi: 10.1029/2007JC004269, 2008.
- 612 van den Broeke, M.,: Strong surface melting preceded collapse of Antarctic Peninsula
613 ice shelf, *Geophys. Res. Lett.*, 32(12), L12815, doi:10.1029/ 2005GL023247,
614 2005.
- 615 Zagorodnov, V., Nagornov, O., Scambos, T. A., A. Muto, A., Mosley-Thompson, E.,
616 Pettit, E. C., and Tyufin, S.: Borehole temperatures reveal details of 20th
617 century warming at Bruce Plateau, Antarctic Peninsula, *The Cryosphere*, 6(3),
618 675–686, doi:10.5194/tc-6-675-2012, 2012.

619 Zgur, F., Rebesco, M., Domack, E. W., Leventer, A., Brachfeld, S., and Willmott, V.:
620 Geophysical survey of the thick, expanded sedimentary fill of the new-born
621 Crane fjord (former Larsen B Ice Shelf, Antarctica), US Geol. Surv. Open File
622 Rep 1047, 2007.

623 Zwally, H., Schutz, R., Hancock, D., and Dimarzio, J., GLAS/ICESat L2 Antarctic and
624 Greenland Ice Sheet Altimetry Data (HDF5). Version 33. Boulder, Colorado
625 USA: NASA DAAC at the National Snow and Ice Data Center,
626 doi:10.5067/ICESAT/GLAS/DATA205, 2012.

627

628 **Table 1. Summary of Mass Balance for the northern Antarctic Peninsula, 2003-2008[†]**
 629 Units: Area (km²), Mean dM/dt (Gt a⁻¹), Number of Measurements, Mean dH/dt (m a⁻¹), Mean dV/dt (km³ a⁻¹)

630	631 Region	Ice-Covered Area	Total dM/dt ^a	Ice Front Retreat			Below 1000 m a.s.l.					Above 1000 m a.s.l.			
				Area ^b	dH/dt ^c	dV/dt ^{d,h}	Area	dDEM ^e	ICESat ^f	dH/dt ^g	dV/dt ^h	Area	ICESat ^f	dH/dt ^g	dV/dt ^h
632	nAP <66°S, 1-33	34222.8	-24.9	325.6	-7.4	-1.2	23571.7	44.8	12476	-1.00	-23.1	10651.7	2668	-0.31	-3.4
633	nAP West, 1-11	14338.2	-4.7	7.8	-3.9	-0.0	9014.3	38.6	2999	-0.27	-2.4	5323.7	893	-0.59	-2.8
634	nAP North, 12-14	3688.0	-2.3	4.0	-3.7	-0.0	3684.3	8.2	2204	-0.69	-2.5	3.7	(0)	(-0.31)	0.0
635	nAP East, 15-33	16196.4	-18.0	313.8	-7.5	-1.2	10872.9	62.4	7279	-1.67	-18.2	5323.5	1775	-0.10	-0.6
636	Northwest AP Coast ⁱ	5255.1	-1.7	--	--	--	3417.9	35.1	1270	-0.27	0.9	1837.0	575	-0.50	-0.9
637	Western IFL Glaciers ^j	679.4	-1.1	11.8	-4.6	-0.0	452.1	35.6	450	-2.24	-1.0	226.5	(0)	-0.84	-0.2
638	Eastern ISL Glaciers ^k	9251.0	-15.2	305.7	-7.7	-1.1	6030.9	70.9	3903	-2.60	-15.7	3232.6	941	-0.01	-0.2
639	James Ross Island ^l	1800.8	-2.4	47.1	-3.3	-0.1	1380.0	58.0	417	-1.93	-2.7	420.7	215	0.02	0.0
640	Prince Gustav tributaries ^m	1885.0	-2.7	58.2	-3.6	-0.1	1478.4	76.6	475	-2.03	-3.0	406.7	123	0.23	0.1
641	Larsen A tributaries ⁿ	3184.4	-4.5	29.3	-2.7	-0.0	2094.8	85.5	1594	-2.32	-4.9	1089.7	329	-0.08	-0.1
642	Larsen B ISL tributaries ^o	4181.6	-8.0	218.2	-9.5	-1.0	2457.7	55.2	1834	-3.18	-7.8	1736.2	489	-0.13	-0.2
643	Scar Inlet Ice Shelf trib. ^p	3524.5	-1.4	--	--	--	2089.8	46.4	1965	-0.47	-0.7	1434.7	715	-0.37	-0.5

644 [†]Data from ICESat and satellite stereo-image differencing. ICESat data span September 2003 – March 2008. Stereo-image DEMs span 2001 to 2010.
 645 Abbreviations for place names: nAP, northern Antarctic Peninsula; ISL, ice shelf loss; IFL, ice front loss.
 646 ^aAssuming mean density of 900 kg/m³ for all dV/dt measurements. Errors for these values are 0.9 times the sum of errors for dV/dt for each row.
 647 ^bArea determined from additional ASTER, SPOT, and Landsat images, spanning 2000-2002 to 2009-2010
 648 ^cRate of elevation loss measured for the first 50 m elevation band above area of grounded ice retreat.
 649 ^dVolume loss assumes flotation was reached midway between 2001 – 2010 (period of observations).
 650 ^ePercent area covered by differential DEM satellite stereo-image data
 651 ^fNumber of repeat-track point measurements used. If <20 ICESat dH/dt measurements are available, the regional mean ICESat dH/dt for areas > 1000 m
 652 (-0.31 m a⁻¹) or, for sub-basins, the main basin mean, is used.
 653 ^gHypsometric weighting for areas below 1000 m elevation.
 654 ^hErrors on dV/dt can be determined by: ±0.3 m a⁻¹ * area for regions ≤1000 m a.s.l. (dDEM and ICESat data) and ±0.15 ma⁻¹ * area for regions >1000 m a.s.l.
 655 (ICESat data)
 656 ⁱGlacier basins 8 – 11
 657 ^jGlacier basins 1a, 4a, 6a, and 12a. Used dDEM data for >1000 m a.s.l. dH/dt estimate
 658 ^kGlacier basins 19, 21-25, 26b, 27-30, and 31a.
 659 ^lGlacier basins 17, 18, and 19
 660 ^mGlacier basins 19 and 21
 661 ⁿGlacier basins 22-25
 662 ^oGlacier basins 26b, 27-30, and 31a
 663 ^pGlacier basins 31b, 32, and 33

664
665
666
667
668
669 **Table 2. Comparison of total mass balance (dM/dt), input surface mass (dM_i/dt), and**
 670 **resulting imbalance ratio.**

671 Units: Area, km²; dM/dt, Gt a⁻¹; Mean dH/dt, m a⁻¹; SMB, kg m⁻² a⁻¹; dM_i/dt, Gt a⁻¹

672	673 Region	Ice-Covered Area	Total dM/dt	Mean dH/dt	Mean SMB	Total dM _i /dt	Imbal. ratio	<1000 dH/dt	<1000 SMB	<1000 dM _i /dt	<1000 ratio	>1000 dH/dt	>1000 SMB	>1000 dM _i /dt	>1000 ratio
674	nAP <66°S, 1-33	34222.8	-24.9	-0.77	1543	54.2	-0.45	-1.00	1295	29.9	-0.70	-0.31	2104	23.1	-0.18
675	nAP West, 1-11	14338.2	-4.7	-0.33	2112	30.4	-0.14	-0.27	1964	17.7	-0.12	-0.59	2361	12.6	-0.17
676	nAP North, 12-14	3688.0	-2.3	-0.69	537	2.0	-1.15	-0.69	537	2.0	-1.15	(-0.31)	920	0.0	--
677	nAP East, 15-33	16196.4	-18.0	-1.20	1268	21.8	-0.81	-1.75	1007	10.5	-1.56	-0.10	1844	9.8	-0.06
678	Northwest AP Coast ^a	5255.1	-1.7	-0.35	2012	10.6	-0.16	-0.27	1770	6.0	0.13	-0.51	2458	4.5	-0.18
679	Western IFL Glaciers ^b	679.4	-1.1	-1.77	1839	1.2	-1.26	-2.24	1484	0.7	-1.29	-0.83	2546	0.6	-0.28
680	Eastern ISL Glaciers ^c	9251.0	-15.2	-1.66	1399	13.0	-1.15	-2.60	1143	6.9	-2.05	-0.07	1898	6.1	-0.04
681	James Ross Island ^d	1800.8	-2.4	-1.44	689	1.2	-2.09	-1.93	653	0.9	-2.70	0.02	834	0.4	0.00
682	Prince Gustav trib. ^e	1885.0	-2.7	-1.54	1173	2.2	-1.23	-2.03	968	1.4	-1.93	0.21	2003	0.8	0.10
683	Larsen A tributaries ^f	3184.4	-4.5	-1.55	1624	5.2	-0.94	-2.32	1358	2.8	-1.58	-0.08	2154	2.3	-0.03
684	Larsen B ISL trib. ^g	4181.6	-8.0	-1.80	1329	5.6	-1.42	-3.18	1064	2.6	-2.68	-0.13	1713	3.0	-0.07
685	Scar Inlet Ice Shelf trib. ^h	3524.5	-1.4	-0.42	1296	4.6	-0.30	-0.47	787	1.6	-0.38	-0.37	2049	2.9	-0.16
686	^a Glacier basins 8 – 11														
687	^b Glacier basins 1a, 4a, 6a, and 12a														
688	^c Glacier basins 19, 21-25, 26b, 27-30, and 31a														
689	^d Glacier basins 17, 18, and 19														
690	^e Glacier basins 19 and 21														
691	^f Glacier basins 22-25														
692	^g Glacier basins 26b, 27-30, and 31a														
693	^h Glacier basins 31b, 32, and 33														

695 **Figures**

696

697 Figure 1. Location and outline of basins and sub-basins in the study area, and sites of
698 two ice cores discussed in the text. Region names, basin numbers, and abbreviations
699 are the same as in Table S2 and S3. Major drainage basins evaluated by the study are
700 outlined in white, sub-basins are indicated in blue. Base image is the MODIS Mosaic
701 of Antarctica (Scambos et al., 2007). Inset, location of the study area shown in Figure
702 2.

703

704 Figure 2. Elevation change rates (dH/dt) and major and minor glacier basin or
705 islands for the northern Antarctic Peninsula study area. Cyan outlines indicate the
706 measured study basins and islands; surrounding numbers and letters refer to Table
707 S2 and S3 entries. Magenta outlines with lower-case labels identify sub-basins
708 within a major basin where a separate hypsometric interpolation is used. Black
709 contour line indicates 1000 m a.s.l. elevation. Major ice shelf retreat areas since
710 1980 (Cook and Vaughan, 2010) are indicated in grey-blue, with years of major
711 collapse events and the limit of extensive grounded ice loss shown. Ice edge is from
712 a 2009 MODIS mosaic (Haran et al., 2014).

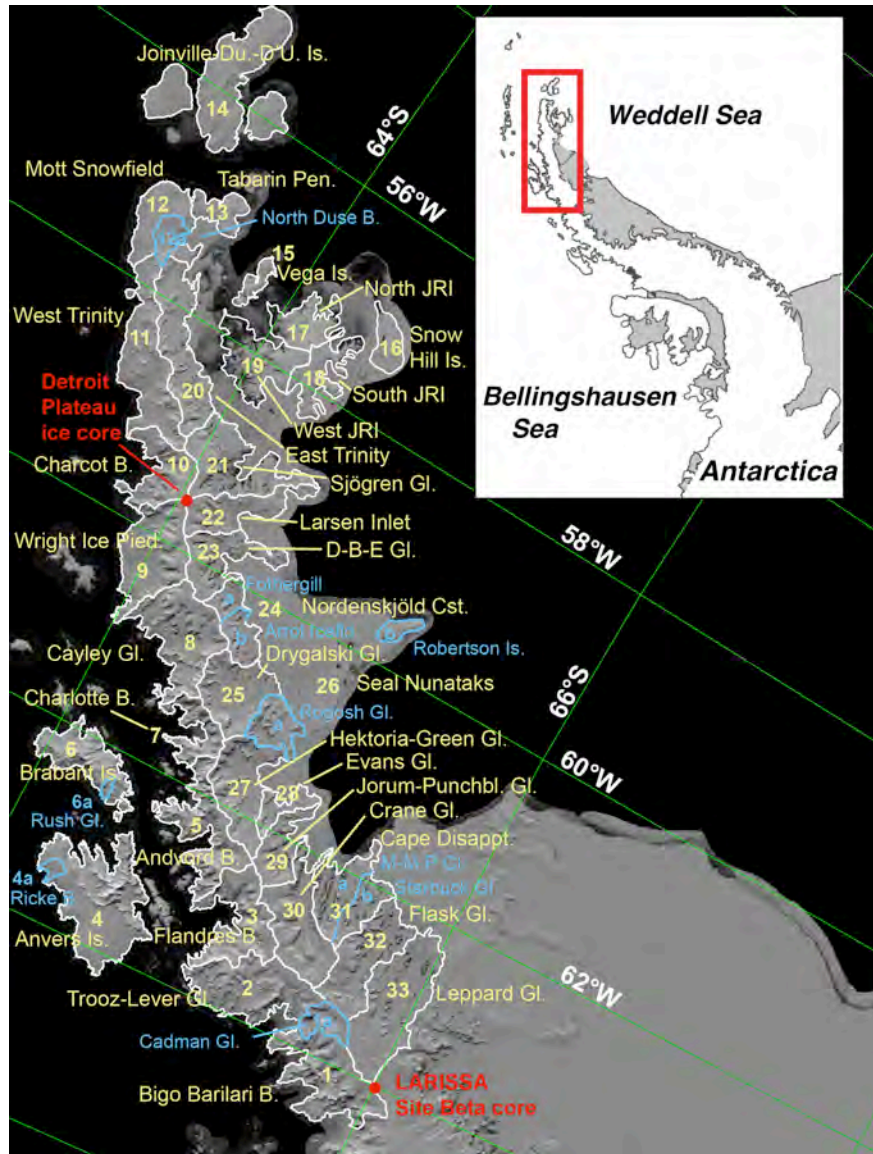
713

714 Figure 3 a-f. Hypsometry of elevation and volume changes of western basins (panel
715 a and b; basins 1 – 11 in Table 1), eastern basins with major ice shelf loss in the
716 period 1986 – 2009 (panels c and d; basins 19, 21-25, and 27-30 in Table 1), and
717 basins draining to the Scar Inlet ice shelf area (panels e and f; basins 31b, 32, and 33
718 in Table 1). Height is binned in 50 m intervals. Note that rates of elevation change
719 trends at the highest elevations (>2000 m a.s.l., right side of left column of panels)
720 are based on few data and are not reliable.

721

722 Figure 4. Comparison of the study area basin extents with RACMO-2 estimated SMB
723 in $\text{kg m}^{-2} \text{a}^{-1}$ (panel a) and mass imbalance ratio for the basin areas separated by
724 high and low elevation areas (above and below 1000 m; panel b).

725



726

727 **Figure 1.** Locations and outlines of basins and sub-basins in the study area, and sites of two
 728 climate ice cores discussed in the text. Region names, basin numbers, and abbreviations are
 729 the same as in Tables S2 and S3. Major drainage basins are outlined in white, sub-basins are
 730 indicated in blue. Base image is the MODIS Mosaic of Antarctica (MOA2004; Scambos *et al.*,
 731 2007; Haran *et al.*, 2005). Inset, location of the study area shown in Figure 2.

732

733

734

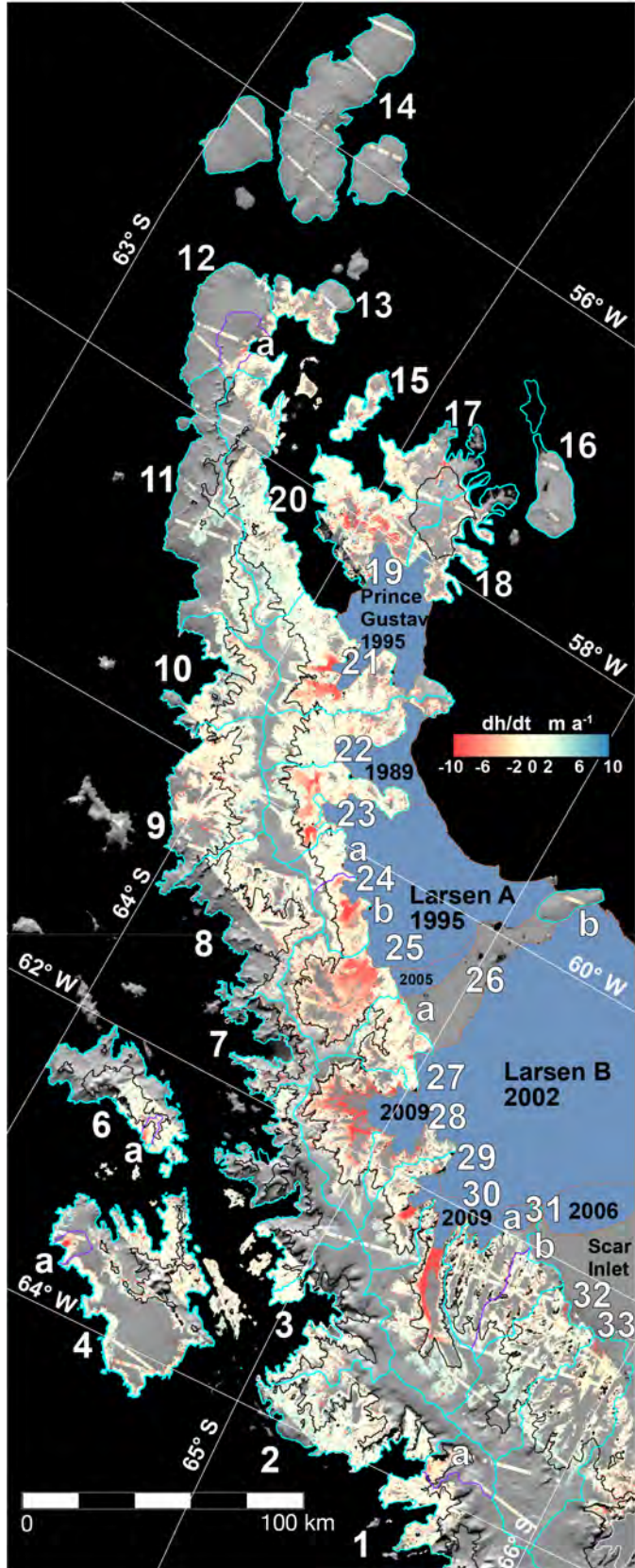
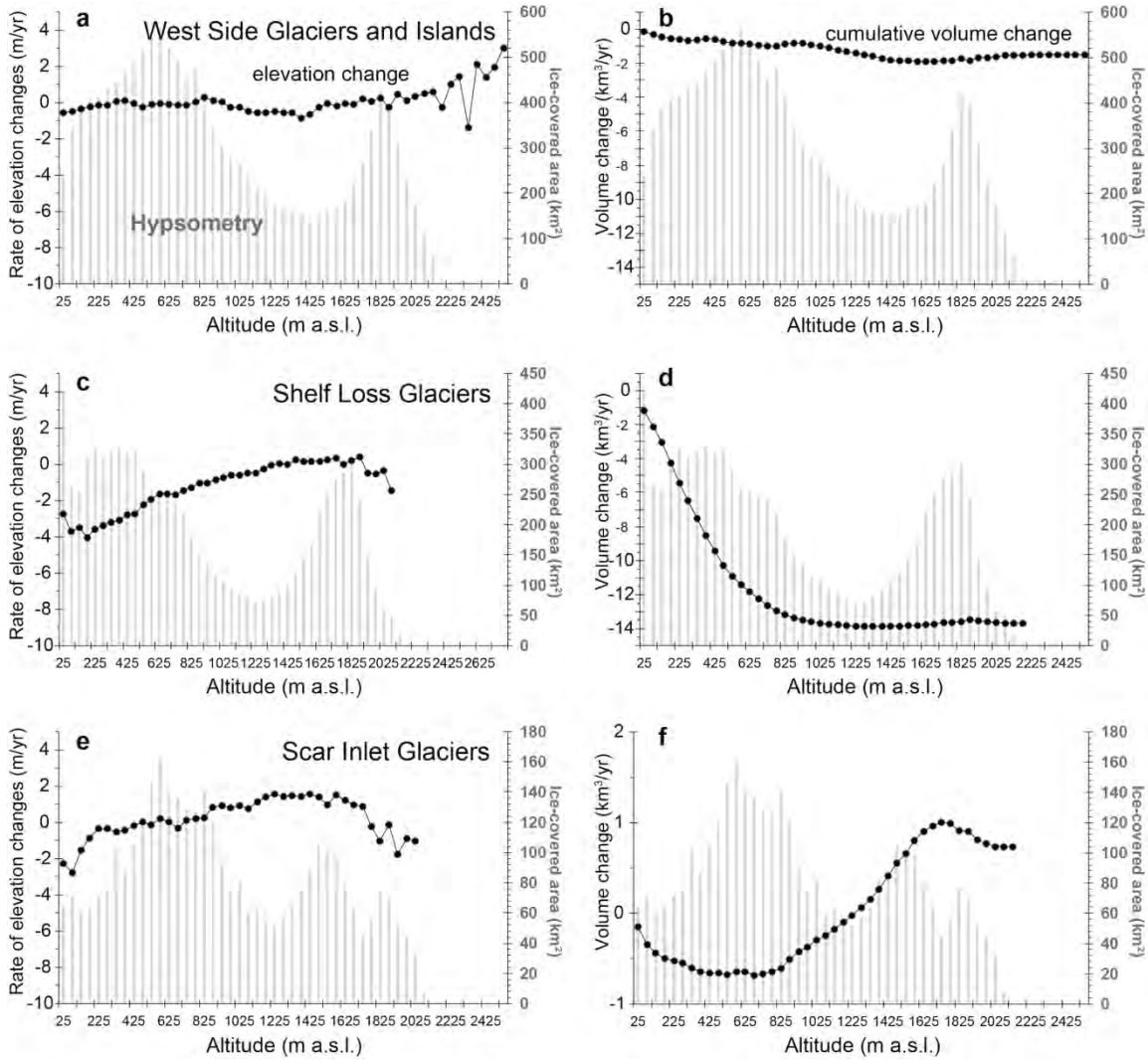


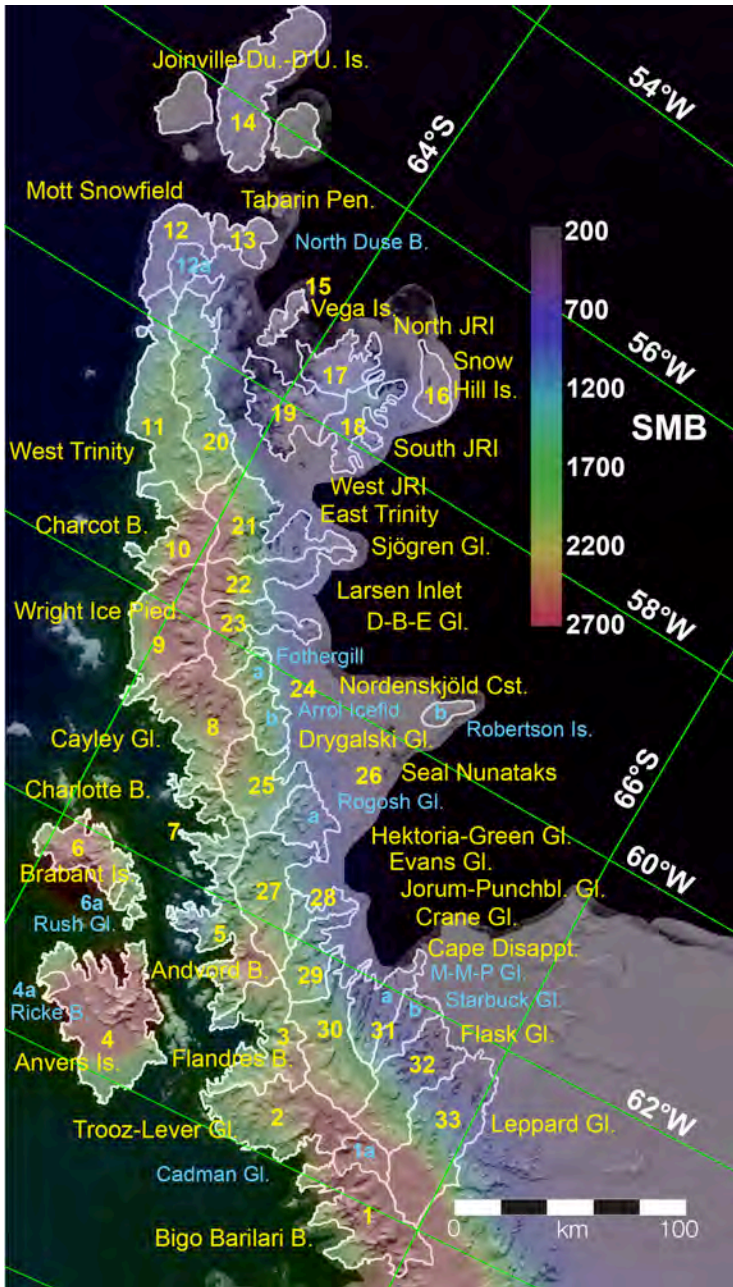
Figure 2. Elevation change rates (dh/dt) and major and minor glacier basin or islands for the northern Antarctic Peninsula study area. Cyan outlines indicate the measured study basins and islands; adjacent numbers and letters refer to Table S2 and S3 entries. Magenta outlines with lower-case labels identify sub-basins within a major basin where a separate hypsometric interpolation is used. A black line indicates the 1000 m a.s.l. elevation contour. Major ice shelf retreat areas since 1980 (*Cook and Vaughan, 2010*) are indicated in blue, with years of major collapse events and the limit of extensive grounded ice loss shown. Ice edge is from a 2009 MODIS mosaic (MOA2009; *Haran et al., 2014*).

736
737
738



739
740
741
742
743
744
745
746
747

Figure 3 a-f. Hypsometry of elevation and volume changes of western nAP basins (panel a and b; basins 1 – 11 in Table S2 and S3), eastern nAP basins with major ice shelf loss in the period 1986 – 2009 (panels c and d; basins 19, 21-25, and 27-30 in Table S2 and S3), and basins draining to the Scar Inlet ice shelf area (panels e and f; basins 31b, 32, and 33 in Tables 1 and 2 and Tables S2 and S3). Height is binned in 50 m intervals. Rates of elevation change trends at the highest elevations (>2000 m a.s.l., right side of left column of panels) are based on few data and are not reliable.



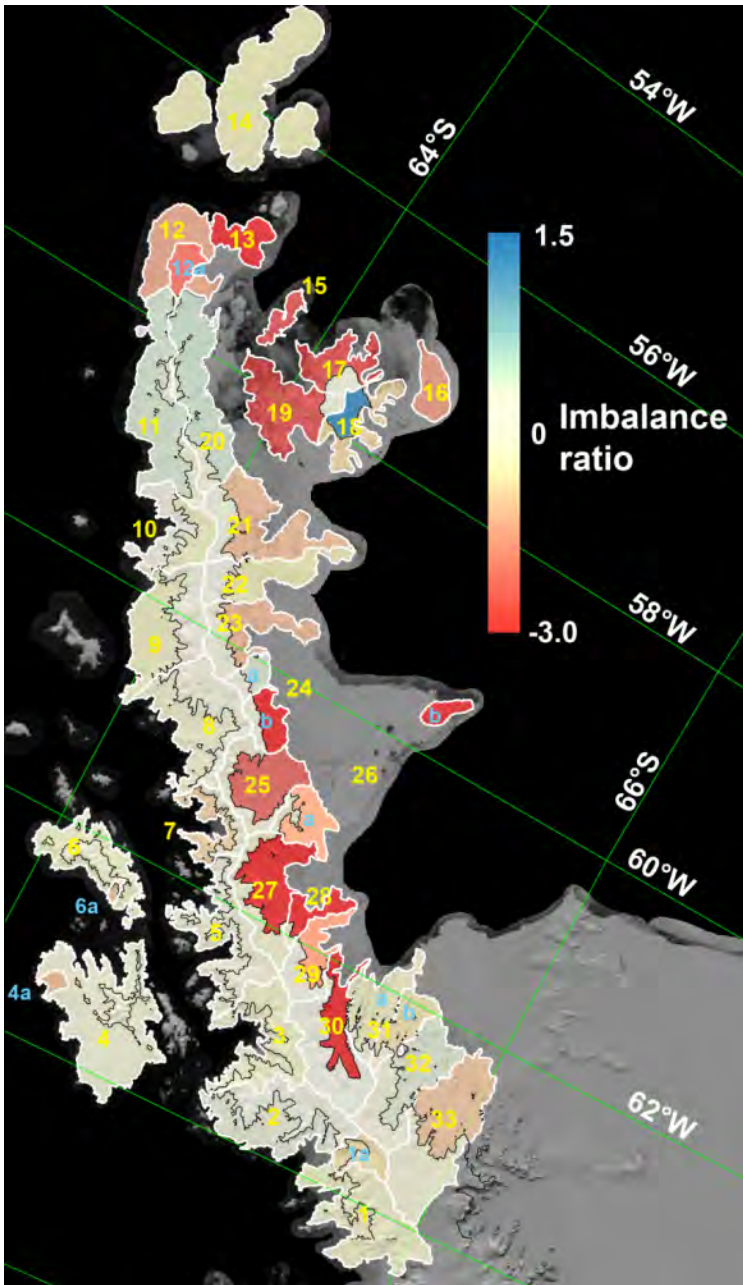
748

749 **Figure 4a.**

750 **Figure 4 a and b.** Comparison of the study area basin extents with RACMO-2
 751 estimated SMB in $\text{kg m}^{-2} \text{a}^{-1}$ (a) and mass imbalance ratio for the basin areas
 752 separated by high and low elevation areas (above and below 1000 m; b).

753

754



755

756 **Figure 4b**

757 **Figure 4 a and b.** Comparison of the study area basin extents with RACMO-2
 758 estimated SMB in $\text{kg m}^{-2} \text{a}^{-1}$ (a) and mass imbalance ratio for the basin areas
 759 separated by high and low elevation areas (above and below 1000 m; b).

1
2 submitted to The Cryosphere Discussions, 04 June 2014;
3 Contact: T. Scambos, teds@nsidc.edu, 303/492-1113

4
5
6
7 **Detailed ice loss pattern in the northern Antarctic Peninsula:**
8 **widespread decline driven by ice front retreats**

9
10
11 Ted A. Scambos¹, Etienne Berthier², Terry Haran¹, Christopher A. Shuman³, Alison J.
12 Cook⁴, Stefan R. M. Ligtenberg⁵, and Jennifer Bohlander¹

13
14 ¹National Snow and Ice Data Center (NSIDC), University of Colorado at Boulder, Boulder CO
15 80303 USA

16 ²Laboratoire d'Etudes en Géophysique et Océanographie Spatiales, Centre National de la
17 Recherche Scientifique (LEGOS CNRS), Université de Toulouse, Toulouse 31400 France

18 ³University of Maryland, Baltimore County, Joint Center for Earth Technology (UMBC JCET)
19 at NASA Goddard Space Flight Center, Greenbelt, MD 20771 USA

20 ⁴Department of Geography, Swansea University, Swansea SA2 8PP UK

21 ⁵Institute for Marine and Atmospheric Research Utrecht (IMAU), Utrecht 3508 TA
22 Netherlands

23
24
25 Corresponding author: T.A. Scambos (National Snow and Ice Data Center, University of
26 Colorado, Boulder, 1540 30th Street Bldg. RL-2, Boulder CO 80303, teds@nsidc.edu, +1-
27 303-492-1113).

28
29

30 **Abstract**

31 The northern Antarctic Peninsula (nAP, <66°S) is one of the most rapidly changing
32 glaciated regions on Earth, yet the spatial patterns of its ice mass loss at the glacier
33 basin scale has to date been poorly documented. We use satellite laser altimetry and
34 satellite stereo-image topography spanning 2001-2010 to map ice elevation change
35 and infer mass changes for 33 glacier basins. Rates of ice volume and ice mass
36 change are $27.7 \pm 8.6 \text{ km}^3 \text{ a}^{-1}$ and $24.9 \pm 7.8 \text{ Gt a}^{-1}$. This mass loss is compatible with
37 recent gravimetric assessments, but it implies that almost all the gravimetry-
38 inferred loss lies in the nAP sector. Mass loss is highest for eastern glaciers affected
39 by major ice shelf collapses in 1995 and 2002, where twelve glaciers account for
40 60% of the total imbalance. However, losses at smaller rates occur throughout the
41 nAP, and at high and low elevation, despite increased snow accumulation along the
42 western coast and at high elevations. We interpret the widespread mass loss to be
43 driven by decades of ice front retreats on both sides of the nAP, and the propagation
44 of kinematic waves triggered at the fronts into the interior.

45 (188 words)

46
47 **Index terms:**

48 Ice Shelves; Glaciers; Mass Balance; Remote Sensing; Instruments and techniques

49 **Keywords:**

50 Antarctic Peninsula; ICESat; DEM differencing; Larsen B; Larsen A; Prince Gustav
51
52
53

54 **1 Introduction**

55 The nAP is one of two key areas of the Antarctic Ice Sheet showing major mass loss,
56 the other being the Pine Island Bay region. Previous studies have shown large
57 negative mass imbalances and significant elevation losses for the nAP (*Ivins et al.*,
58 2011; *Shepherd et al.*, 2012; *Luthcke et al.*, 2013; *Sasgen et al.*, 2013; *Shepherd et al.*,
59 2014), but in general these have not resolved the spatial distribution of the mass
60 balance change in detail. Studies based on gravitational change detection using the
61 Gravity Recovery and Climate Experiment satellite system (GRACE) have an
62 inherent spatial resolution of roughly 250 km scale (*Ivins et al.*, 2011; *Shepherd et*

63 *al.*, 2012; *Luthcke et al.*, 2013; *Sasgen et al.*, 2013), far larger than the scale of the
64 nAP individual glacier basins and islands. Past altimetry-based studies (*Pritchard et*
65 *al.*, 2009; *Flament and Rémy*, 2012; *Shepherd et al.*, 2012) suffer from either sparse
66 coverage or slope correction issues, or both, due to the steep terrain in the nAP. In
67 the published assessments based on laser altimetry (*Shepherd et al.*, 2012), severe
68 assumptions and large extrapolations are required to interpolate the data across the
69 entire region. Mass budget methods (*Rignot et al.*, 2004, 2008; *Rott et al.*, 2011;
70 *Shepherd et al.*, 2012), which aim to difference ice outflow and surface mass balance
71 (SMB) over each glacier basin have to date shown results that are difficult to
72 reconcile with other studies of the same glaciers (*Shuman et al.*, 2011; *Berthier et al.*,
73 2012). This is primarily due to spatially coarse SMB estimates from models or field
74 measurements, difficulties in estimating the cross-sectional area of the glaciers, and
75 differences in the span of time used to estimate ice flux changes (*Berthier et al.*,
76 2012).

77
78 The goal of this study is to determine the spatial pattern of ice elevation changes in
79 the nAP, improve estimates of mass balance for the region, and study the
80 relationship of mass balance with ice shelf collapse and ice front retreats in the area.
81 In light of known climate changes in the region, such as air warming, regional sea ice
82 decline, and increasing accumulation (e.g., *Mulvaney et al.* 2012; *Zagorodnov et al.*,
83 2012; *Stammerjohn et al.*, 2008; *Lenaerts et al.*, 2012), our study reveals a pattern of
84 ice mass loss in space and (we infer) time that may represent the characteristics of
85 mass loss in other areas of Antarctica in the coming century.

87 **2 Methods**

88 Our study combines satellite stereo-image digital elevation model differencing
89 (dDEM) with repeat-track laser altimetry from the Ice, Cloud and land Elevation
90 Satellite (ICESat; *Shutz et al.*, 2005), with the objective of providing an assessment of
91 vertical movement resolved at the scale of the major glacier catchments. We use
92 stereo-image data from Advanced Spaceborne Thermal Emission and Reflection
93 Radiometer (ASTER; *Fujisada et al.*, 2005) and Satellite Pour l'Observation de la

94 Terre 5 (SPOT5; *Korona et al.*, 2009). Eight satellite stereo-image data sets from the
95 ASTER sensor, and six from the SPOT-5 Haute Resolution Systeme (HRS) sensor
96 (Table S1 and Figure S1) were processed using previously published methods
97 (*Shuman et al.*, 2011; *Berthier et al.*, 2012; *Gardelle et al.*, 2013).

98

99 For the ICESat repeat-track data (Release 633), we used 26 orbit ground tracks from
100 the 91-day-repeat orbit crossing the nAP and major ice-covered islands for the high-
101 energy laser campaigns (ICESat Laser 2A through Laser 3J, September 2003 – March
102 2008; *Shuman et al.*, 2006). Cross-track elevation adjustment and along-track
103 filtering are used to improve measurement quality, based on surface slopes (not
104 elevations) derived from a recent Antarctic Peninsula DEM (*Cook et al.*, 2012). We
105 first eliminated ICESat profile tracks more than 300 meters from the reference track
106 position, and sections where the absolute slope from the gridded DEM was $> \pm 10^\circ$
107 for the reference track or campaign profile location, or $> \pm 5^\circ$ slope along-track for
108 both the measurement track and reference track. We further required the profile's
109 elevation data to be within 50 m (vertically) of the gridded DEM elevation values. All
110 elevations are referenced to the EGM96 geoid datum. To migrate the track data to
111 the reference track and compare elevations, we identified reference track 'stations'
112 every 43.75 m along the reference track (one-fourth the distance between ICESat
113 altimetry shot locations along track). We then applied an elevation correction based
114 on the difference between the interpolated gridded DEM elevation at the nearest
115 reference track station and the ICESat track data point. ICESat campaign data were
116 compared by differencing their migrated elevations, divided by the time in years
117 between dates of track acquisition. To reduce effects of possible seasonal variations
118 in elevation, we compared only near-integer-year separated repeat profiles, e.g.,
119 data from campaigns 2A to 3A (~October, ~1 year apart) or 3B to 3H (~March, ~2
120 years apart).

121

122 To evaluate different processes in elevation and ice mass change, we treat regions
123 above and below 1000 m above sea level (a.s.l.) separately for each of 33 drainage
124 basins. This is the approximate elevation of an extensive escarpment in the nAP

125 separating a plateau area from individual glacier cirques. Above 1000 m a.s.l., and
126 for islands without sufficient dDEM coverage (Robertson Is., Snow Hill Is., and
127 Joinville, Dundee, and D'Urville Is.; Figure 1), the rate of elevation change (dH/dt) is
128 determined from satellite laser altimetry alone. In smooth high elevation areas,
129 correlation of satellite stereo-images often fails due to a lack of high-contrast
130 surface features of sufficient horizontal scale (tens of meters). Below 1000 m a.s.l., a
131 hypsometric interpolation method was applied to individual glaciated basins to
132 extend differencing of satellite stereo-image DEMs (dDEM) and ICESat dH/dt
133 measurements to areas not directly measured. ICESat dH/dt was weighted 10-fold
134 relative to dDEM dH/dt to prevent small image areas from dominating the dH/dt
135 mapping and to reflect the higher accuracy of individual ICESat-based
136 measurements, using

137

$$138 \quad (dH/dt_{DEM} * (N_{DEM}/e_{DEM}) + dH/dt_{ICESat} * (N_{ICESat}/e_{ICESat})) / ((N_{DEM}/e_{DEM}) + (N_{ICESat}/e_{ICESat})) \quad (1)$$

139

140 where N is the number of measurements (50 m grid cells for the dDEMs; shot point
141 locations at the 43.75 m spacing for ICESat) and e is an inverse weighting of the
142 measurement methods. For dDEMs we used a weight of 1, and for ICESat, we used
143 0.1. This allowed the fewer but more accurate ICESat-based measurements to
144 contribute to the final result in basins with extensive dDEM coverage. ICESat data
145 was often in regions not well covered by dDEM results.

146

147 We also estimate the above-flotation mass loss of grounded-ice areas that retreated
148 at least 2 km² during the study interval (2001-2010), as identified by image
149 mapping (Cook *et al.*, 2005; Cook and Vaughan, 2010). To estimate the volume and
150 mass loss represented by these areas we mapped the area of retreat during our
151 study period (2002-2010) and half the mean elevation loss rate observed just above
152 the area of grounded ice retreat. This represents an assumption that the vertical
153 elevation change rate of the retreated ice was identical to the region just upstream
154 of the loss area, and that the time of ice front retreat (e.g., when the ice calved and
155 drifted away) was midway through the study period.

156

157 Errors for our assessment of dH/dt (Tables 1 and S2), are based on past analysis of
158 the dDEM method (*Shuman et al., 2011; Berthier et al., 2012*), on inter-comparisons
159 of the two methods at sites having both dDEM and ICESat measurements, and on
160 crossover analysis of ICESat cross-track-corrected data (Table S4). Past analysis for
161 this region suggests that dDEM methods using mixed ASTER and SPOT5 imagery
162 can have a ± 5 m uncertainty for individual glacier basin, i.e. ~ 1 m a^{-1} given a 5-yr
163 time separation between DEMs. However, examining our ICESat and dDEM dH/dt at
164 sites with both measurements (6158 sites) shows that the methods differ by just
165 ~ 0.3 m a^{-1} overall, and range between 0.07 to 0.75 m a^{-1} over various sub-sets of our
166 measurements (Table S4). This is in agreement with our previous study that showed
167 reduced errors when dDEM results are averaged over basin-scale areas (*Berthier et*
168 *al., 2012*). Seven crossover sites with slope-corrected ICESat dH/dt measurements
169 show good agreement with the dDEM measurements at the same locations (mean
170 offset of $+0.05$ m a^{-1}).

171

172 Errors in the ICESat cross-track correction for dH/dt are more dependent on slope
173 errors in the gridded Cook et al. DEM and not its absolute elevation accuracy.
174 Assuming our selection criteria eliminated regions of significant error in the gridded
175 DEM, we estimate that across-track or along-track slopes in the Cook et al. DEM are
176 accurate to within $\pm 0.5^\circ$, or ± 8.5 m km^{-1} . A test of this was conducted by comparing
177 the Cook et al. DEM slopes with a DEM acquired in 2009 by the NASA Land,
178 Vegetation, and Ice Sensor (LVIS) airborne laser altimeter, covering about 20% of
179 the study region. This showed that the mean difference in along-track slope in the
180 overlap region was $0.05 \pm 1.2^\circ$ when our criteria are applied to both data sets. For
181 laser altimetry measurements alone, our inferred mean slope error of $\pm 0.5^\circ$ implies
182 a mean laser measurement pair cross-track correction error of ± 1.28 m (assuming a
183 mean cross-track distance of 150 m). We assume this error is randomly distributed
184 when averaging a glacier basin. Thus for the average of 20 measurement sites, the
185 mean error is < 30 cm. Since laser measurement pairs may have 1 to 4 years
186 separation in time, our overall mean error in elevation change rate is significantly

187 less than this. Additionally, the majority of the basins we consider have $\gg 20$
188 measurement sites.

189

190 Considering all sources of error, and variations in the time-span of measurements
191 for dDEM and ICESat measurements, data density variations for the basins, and the
192 strong agreement between these independent altimetric methods, We adopt a mean
193 error of $\pm 0.15 \text{ m a}^{-1}$ for regions of laser altimetry measurement alone (above 1000
194 m a.s.l.), and $\pm 0.3 \text{ m a}^{-1}$ for our dDEM plus altimetry measurements (below 1000 m
195 a.s.l.) and the glacier basins, islands, and sub-basins without laser altimetry. Errors
196 for volume and mass change determinations thus scale with area.

197

198 **3 Results**

199 An overview of our results is shown in Figure 2 and Table 1, and detailed basin-by-
200 basin values and patterns are provided in supplementary Table S2. The results show
201 that basins impacted by recent ice shelf loss and ice front retreat have very high
202 rates of change, but also indicate that few areas — high or low, east or west — have
203 positive dH/dt . Ice-shelf loss (ISL) basins, all on the eastern side of the nAP, and four
204 smaller areas of grounded ice front loss (IFL) on the western and northeastern side
205 of the nAP, show a characteristic pattern of very high elevation loss rates just
206 upstream of the ice front but far lower elevation losses at high elevation. Mean
207 elevation change for areas below 1000 m a.s.l. at 12 eastern-side ISL glacier basins
208 (or sub-basins) is -2.6 m a^{-1} (range, $+0.4$ to -5.8 m a^{-1}) and -2.2 m a^{-1} (-2.0 to -2.7 m a^{-1})
209 for the four western-side and northeastern IFL sub-basins experiencing recent ice
210 front retreat ($>2 \text{ km}^2$ since 2000). At elevations $>1000 \text{ m}$, elevation loss in all the
211 eastern ISL basins is small ($\sim -0.10 \text{ m a}^{-1}$). Glacier systems on the western nAP coast
212 and the western islands below 1000 m a.s.l., excluding the recent IFL regions, are
213 changing at variable rates (typically $\sim -0.15 \text{ m a}^{-1}$, range $+0.7$ to -1.6 m a^{-1}). However,
214 these western-side basins are losing elevation at significant rates above 1000 m a.s.l.
215 (mean of -0.59 m a^{-1}).

216

217 We examine the rates of surface elevation change and cumulative ice volume change

218 as they vary with altitude for three sub-regions of the study area in Figure 3. The
219 patterns of elevation change with altitude illustrate the differences between the
220 western-side glacier and island regions and the eastern-side ISL areas, and also
221 highlight the bi-modal hypsometry pattern characteristic of the nAP. Eastern-side
222 ISL areas show dramatically decreasing elevation with time, and large volume
223 changes at low elevations, and little or no significant change in the upper-most
224 catchment areas (Figure 3c-d). Western-side glaciers show mildly negative rates of
225 elevation change at all elevations, and a steady cumulative volume decrease rate
226 with altitude. The major glaciers of Scar Inlet Ice Shelf, the lone remaining large
227 (>50 km²) ice shelf in the study area with significant tributary glaciers, show a
228 unique pattern of ice losses at low elevation and some areas of thickening at
229 altitude. We believe this is likely the pattern of elevation change present for the
230 eastern nAP ISL glacier systems in the years prior to shelf disintegration.

231

232 **4 Discussion**

233 The widespread elevation losses suggested here for both sides of the nAP at high
234 elevations, and especially for the western side of the divide, have significant
235 implications for its recent mass change history. Previous observational studies have
236 shown that the elevation decline pattern for ISL or IFL glaciers migrates upstream
237 and diffuses on a scale of years to decades (*Howat et al., 2007; Joughin et al., 2008;*
238 *Shuman et al., 2011; Berthier et al., 2012*), consistent with kinematic wave models of
239 glacier response to ice front stress changes for tidewater glaciers (*Pfeffer, 2007;*
240 *Nick et al., 2009; Favier et al., 2014*). In past work (*Shuman et al., 2011; Berthier et*
241 *al., 2012*) and in these results we observe that eastern ISL glaciers are currently
242 propagating kinematic waves upstream from their lower trunk areas, but this
243 process has not yet had a significant impact on higher elevations. Western-coast
244 nAP glacier front retreats, elevation losses, and accelerations have been
245 documented (*Cook and Vaughan, 2005; Pritchard and Vaughan, 2007; Kunz et al.,*
246 *2012*), with a major pulse of retreat beginning in the 1970s. These losses and earlier
247 ones (e.g., *Crist et al., 2014 in press*) appear to have now propagated throughout the
248 entirety of the western basins, leading to significant and widespread surface

249 lowering.

250

251 However, any measurement of elevation or mass losses along the western coast and
252 in the upper elevation areas must be reconciled with a large recent positive
253 accumulation anomaly. Ice cores at two sites on the nAP ridge crest (Detroit Plateau,
254 64.08°S, 59.65°W, 1937 m a.s.l., and Site Beta of the Larsen Ice Shelf System,
255 Antarctica, 66.03°S, 64.04°W, 1980 m a.s.l.; Figure 1) show significant increases in
256 accumulation in the late 20th century: 2052 to 2776 kg m² a⁻¹ from 1981-87 to 2001-
257 07, and 1750 to 2710 kg m² a⁻¹ from 1960-69 to 2000-08, respectively (*Potocki et al.*,
258 2011; *Goodwin*, 2013). Models of precipitation input for the region (*Saha et al.*,
259 2010; *Dee et al.*, 2011; *Lenaerts et al.*, 2012) also show a strong overall increase for
260 the most recent decades, but some indicate a slight decline the last decade, covering
261 our dH/dt measurement period (*Saha et al.*, 2010; *Lenaerts et al.*, 2012; *Shepherd et*
262 *al.*, 2012). The large increase and later reduction in accumulation are associated
263 with multi-decadal warming (*Barrand et al.*, 2013) and associated reductions in sea
264 ice extent northwest of the nAP (*Stammerjohn et al.*, 2012) recently moderated by a
265 slight cooling trend (*Blunden and Arndt*, 2012; *Zagorodnov et al.*, 2012).

266

267 Multi-decadal accumulation, temperature and snowmelt trends cause changes in the
268 compaction rate of snow and firn, and can potentially impact measurements of
269 surface elevation change (*Ligtenberg et al.*, 2011). Using a model climate time series
270 (based on reanalysis of weather data) spanning the period of our measurements
271 (RACMO-2.1/ANT; *Lenaerts et al.*, 2012), a dH/dt for the firn column at 27 km
272 spatial scale is obtained similar to that used in previous related analyses (*Pritchard*
273 *et al.*, 2012; *Gardner et al.*, 2013). The modeled inter-annual variability in
274 accumulation, temperature and snowmelt, and their effect on firn compaction result
275 in dH/dt corrections between -0.19 to +0.12 m a⁻¹ on the grounded ice of the nAP,
276 with generally positive (thickening) corrections on the western side and negative to
277 the east. The small effect on the firn layer, and the high variability of accumulation
278 both inter-annually and among the basin areas (Figure 4a) make the correction
279 relatively insignificant. We therefore report dH/dt as observed from the satellite

280 data. From these observations, we report mass change in Table 1 and Table S2 as:

281

$$282 \quad (dH/dt)_{\text{hyps}} * (A) * r \quad (2)$$

283

284 where $(dH/dt)_{\text{hyps}}$ is the elevation-band-weighted mean measured dH/dt , A is area
285 of the glacier basin or island, and r is our assumed mean density of ice and firn lost
286 by dynamics (900 kg m^{-3}). We eliminated the nunatak areas from each of the basins,
287 based on the Antarctic Digital Database mapping of rock outcroppings in the region
288 similar to previous studies (e.g., *Gardner et al.*, 2013).

289

290 Our estimate of mass balance for the combined nAP region is $-24.9 \pm 7.8 \text{ Gt a}^{-1}$, with
291 the great majority of the mass loss occurring at elevations below 1000 m a.s.l. ($-$
292 $21.9 \pm 6.3 \text{ Gt a}^{-1}$, or 88%; Table 1). Regionally, the eastern nAP basins dominate the
293 mass loss at $-17.7 \pm 3.7 \text{ Gt a}^{-1}$, or 72% of the loss, and of this, $-15.0 \pm 3.2 \text{ Gt a}^{-1}$ (60%) is
294 from 12 glacier basins flowing into embayments formerly occupied by the Prince
295 Gustav, Larsen Inlet, Larsen A, and Larsen B ice shelves. For the 11 western nAP
296 glacier basins and islands, the mass loss rate at high elevation is indistinguishable
297 from losses lower and near the coast ($-2.3 \pm 0.7 \text{ Gt a}^{-1}$ $>1000 \text{ m a.s.l.}$, and $-2.2 \pm 1.0 \text{ Gt}$
298 a^{-1} below). Overall, the nAP region accounts for $\sim 29\%$ of Antarctica mass imbalance
299 during the study period⁴.

300

301 We also examined the mass balance ratio of the basins and regional areas, based on
302 mass input, primarily snow accumulation (*Lenaerts et al.*, 2012; Table 2, Table S3).
303 Mass accumulation from the model (surface mass balance, or SMB) in the region has
304 a very large gradient from west to east, with values of 1500 to $3000 \text{ kg m}^{-2} \text{ a}^{-1}$ for
305 the western areas and high elevations dropping to ~ 500 to $1500 \text{ kg m}^{-2} \text{ a}^{-1}$ in the
306 low elevation areas of the eastern nAP coast. A ratio of the mass balance divided by
307 the mass accumulation input indicates the degree of imbalance in the glacier
308 systems, and suggests the level of ice flux increase for glacier systems having
309 recently accelerated due to ice front or ice shelf losses. We term this value the
310 imbalance ratio. The imbalance ratio for the nAP as a whole is -0.45 , implying that

311 mass outflow is 45% greater during the study period relative to a steady-state rate
312 in the current climate. For the eastern nAP glaciers, the ratio is -0.3 to -3.2 (average,
313 -0.8) with the major ISL glaciers in the Larsen A and Larsen B between -0.33 and -
314 3.4. The upper areas of these glacier systems are essentially balanced (\sim -0.1). IFL
315 glaciers along the western and northern coastlines have imbalance ratios similar to
316 the ISL glaciers, \sim -0.5 to -2.4.

317

318 Our mass balance estimate for the nAP region agrees well with recently published
319 values, although in some cases we believe this is coincidental. Recent GRACE-based
320 estimates that can be most easily compared with our study yield values of -27.5 ± 10
321 Gt a^{-1} (summing the mascons encompassing and adjacent to our study area)
322 (*Luthcke et al.*, 2013), and $26 \pm 3 \text{ Gt a}^{-1}$ for a larger GRACE mascon extending to 70°S
323 (*Sasgen et al.*, 2013). Both these GRACE-derived results inherently include portions
324 of the Larsen C Ice Shelf and adjacent ice-covered islands we did not measure
325 (notably, King George Island) that lost elevation and mass during the ICESat period
326 (*Gardner et al.*, 2013) due to the low spatial resolution of the GRACE gravimetric
327 measurement. Similarly, the strong east-west gradient revealed in our study is not
328 discernable by the GRACE system. Overall, however, the GRACE results provide a
329 good summary confirmation for our study, and imply that nearly all of the mass loss
330 for the Peninsula lies in a relatively small part of the Peninsula ice sheet
331 (specifically, the nAP region defined here).

332

333 For earlier ICESat-only studies of the mass balance in the area (*Shepherd et al.*,
334 2012), the apparent agreement is likely fortuitous. Simple extrapolation methods
335 that do not include information about individual basin dynamics (e.g.,
336 spatial/elevation extent, ice shelf loss, east-west variations), lead to very different
337 values for total mass change. We conducted two experiments using our cross-track
338 adjusted ICESat data alone to examine the scale of possible discrepancies. With an
339 assumption of uniform mean elevation change for each elevation band throughout
340 the nAP the volume change from ICESat data would be $-36.6 \text{ km}^3 \text{ a}^{-1}$. This
341 overestimate derives from ISL glaciers forming too great a part of the net elevation

342 change measurement data, especially for their lower elevations. This is, in part, due
343 to more ICESat data being acquired along the eastern nAP, likely a result of less
344 cloud cover there. If one partially addresses this by separating ISL basins, the
345 volume change is still 10% greater than our study, $-30.6 \text{ km}^3 \text{ a}^{-1}$.

346

347 The most recent assessment of the mass balance of the Peninsula as of this writing
348 uses CryoSat-2 interferometric radar altimetry data to infer a mass balance of $-$
349 $23 \pm 18 \text{ Gt a}^{-1}$ for a period following our evaluation, 2010-2013 (McMillan et al.,
350 2014). The agreement is well within both studies' error bars, and suggests that mass
351 balance for the Peninsula is not decreasing significantly at the present time.

352

353 We now examine the potential impact of further ice shelf loss in the Scar Inlet
354 region, a remnant ice shelf section from the Larsen B Ice Shelf. Comparing high-
355 resolution bathymetric mapping of the seabed exposed by nAP-wide ice shelf loss
356 and glacier retreat with our data in Figure 1 shows that it is the glaciers with deep
357 ($>500 \text{ m}$) troughs and recent ice shelf loss that have the greatest elevation loss and
358 mass imbalance (Zgur et al., 2007; Shuman et al., 2011; Rebesco et al., 2014
359 submitted). Recent ice-thickness maps of the tributary glaciers (Starbuck, Flask, and
360 Leppard glaciers) of the still- intact Scar Inlet ice shelf (SIIS) indicate they have
361 unusually deep glacier troughs just behind the grounding line, well in excess of 1000
362 m below sea level in the case of Flask Glacier, and -500 m a. s. l. for Starbuck glacier
363 (Farinotti et al., 2013, Farinotti et al., 2014). From Table S5, the mean imbalance
364 ratio of ISL glaciers with ice-front bathymetric troughs exceeding 500 m depth is $-$
365 1.20, and -3.18 for regions $<-1000 \text{ m a.s.l.}$ (for comparison, it is $+0.07$ for trough
366 areas $>-500 \text{ m a.s.l.}$). If we assume that the three primary tributary glaciers of SIIS
367 will experience the same mean imbalance ratio following a collapse of their frontal
368 ice shelf in Scar Inlet, we can anticipate increased mass imbalance in those basins,
369 from -1.36 Gt a^{-1} during our study period to $\sim -5.5 \text{ Gt a}^{-1}$.

370

371 **5 Conclusions**

372 Overall, our study suggests that the nAP mass imbalance pattern is a combination of

373 several recent changes to the coastal glaciers and ice shelf systems, likely beginning
374 several decades ago along the western coastal fjords and islands, with extensive
375 inland propagation of mass loss to the ice divide area, and more recent ice shelf loss
376 along the eastern flanks and islands with extensive and expanding inland
377 propogation. Further, the measured large increase in snow accumulation in the past
378 few decades has not created large regions of positive mass balance suggesting that
379 negative mass balances will continue into the future.

380

381 **Acknowledgements**

382 The ICESat data for this paper are available at the NASA Distributed Active Archive
383 Center at NSIDC (GLA12 - GLAS/ICESat L2 Antarctic and Greenland Ice Sheet
384 Altimetry Data). The SPOT5 HRS data were provided at no cost by CNES through the
385 SPIRIT project. The ASTER data were provided at no cost by NASA/USGS through
386 the Global Land Ice Measurements from Space (GLIMS) project. This work was
387 supported by NASA grant NNX10AR76G to T. Scambos and W. Abdalati, the TOSCA
388 and ISIS programs of the French Space Agency (CNES) to E. Berthier, NASA
389 Cryospheric Program funds to C. Shuman, and NSF grant ANT-0732921 to T.
390 Scambos, and the Netherlands Polar Program and European Union Seventh
391 Framwork Programme, grant 226375 to S. Ligtenberg.

392

393 *T. Scambos led the writing and compilation of graphics and tables, and with T. Haran and J.*
394 *Bohlander, conducted the ICESat-based elevation change analysis. E. Berthier conducted the*
395 *differential DEM analysis and integrated the ICESat data with the dDEM data. C. Shuman and*
396 *A. Cook evaluated glacier front area changes and C. Shuman produced components of Figure 3.*
397 *A. Cook provided the glacier basin outlines. S. Ligtenberg evaluated the firn compaction and*
398 *accumulation variability estimates, and their impact on our results. All co-authors contributed*
399 *to the writing of the paper.*

400

401

402

403

404 **References**

405
406
407
408
409

410
411
412

413
414

415
416
417

418
419
420

421
422
423
424

425
426
427
428

429
430
431

432
433
434
435

436
437
438
439

Barrand, N. E., Vaughan, D. G., Steiner, N., Tedesco, M., Kuipers Munneke, P., van den Broeke, M. J., and Hosking, J. S.: Trends in Antarctic Peninsula surface melting conditions from observations and regional climate modeling, *J. Geophys. Res.*, 118(1), 315–330, doi:10.1029/2012JF002559, 2013.

Berthier, E., Scambos, T. A., and Shuman, C. A.: Mass loss of Larsen B tributary glaciers (Antarctic Peninsula) unabated since 2002, *Geophys. Res. Lett.*, 39 L13501, doi:10.1029/2012GL051755, 2012.

Blunden, J., and Arndt, D. S.: State of the Climate in 2011, *Bull. Amer. Meteor. Soc.*, 93(7), S1–S282, doi:10.1175/2012BAMSStateoftheClimate.1., 2012.

Cook, A. J., and Vaughan, D. G.: Overview of areal changes of the ice shelves on the Antarctic Peninsula over the past 50 years, *The Cryosphere*, 4(1), 77–98, doi:10.5194/tc-4-77-2010, 2010.

Cook, A. J., Fox, A. J., Vaughan, D. G., and Ferrigno, J. G.: Retreating glacier fronts on the Antarctic Peninsula over the past half-century, *Science*, 308(5721), 541–544, 2005.

Cook, A. J., Murray, T., Luckman, A., Vaughan, D. G., and Barrand, N. E.: A new 100-m Digital Elevation Model of the Antarctic Peninsula derived from ASTER Global DEM: methods and accuracy assessment, *Earth System Science Data*, 4, 129–142, doi:10.5194/essd-4-129-2012, 2012.

Crist, A., Talia-Murray, M., Elking, N., Domack, E., Leventer, A., Lavoie, C., Brachfield, S., Yoo, K.-C., Gilbert, R., Jeong, S.-M., Petrushak, S., Wellner, J., et al.: Late Holoceneglacial advance and ice shelf growth in Barilari 1 Bay, Graham Land, west Antarctic Peninsula, *Geol. Soc. Am. Bull.*, 2014 in press.

Dee, D. P. et al.: The ERA-Interim reanalysis: configuration and performance of the data assimilation system, *Q. Jour. Royal Met. Soc.*, 137(656), 553–597, doi:10.1002/qj.828, 2011.

Farinotti, D., Corr, H., and Gudmundsson, G. H.: The ice thickness distribution of Flask Glacier, Antarctic Peninsula, determined by combining radio-echo soundings, surface velocity data and flow modelling, *Ann. Glaciol.*, 54(63), 18–24, doi:10.3189/2013AoG63A603, 2013.

Farinotti, D., King, E. C., Albrecht, A., Huss, M., and Gudmundsson, G. H.: The bedrock topography of Starbuck Glacier, Antarctic Peninsula, as measured by radio-echo sounding, *Ann. Glaciol.*, 55(67), 22–28, doi:10.3189/2014AoG67A025, 2014.

- 440 Favier, L., Durand, G., Cornford, S. L., Gudmundsson, G. H., Gagliardini, O., Gillet-
441 Chaulet, F., Zwinger, T., Payne, A. J., and Le Brocq, A. M.: Retreat of Pine Island
442 Glacier controlled by marine ice-sheet instability, *Nature Clim. Change*, 4(2),
443 117–121, doi:10.1038/nclimate2094, 2014
- 444 Flament, T., and Rémy, F.: Dynamic thinning of Antarctic glaciers from along-track
445 repeat radar altimetry, *J. Glaciol.*, 58(211), 830–840,
446 doi:10.3189/2012JoG11J118, 2012.
- 447 Fujisada, H., Bailey, G. B., Kelly, G. G., Hara, S., and Abrams, M. J.: ASTER DEM
448 performance, *IEEE T. Geosci. Remote Sens.*, 43(12), 2707–2714, 2005
- 449 Gardelle, J., Berthier, E., Arnaud, Y., and Käab, A.: Region-wide glacier mass balances
450 over the Pamir-Karakoram-Himalaya during 1999–2011, *The Cryosphere*, 7,
451 1263–1286, doi:10.5194/tc-7-1263-2013, 2013.
- 452 Gardner, A. S., Moholdt, G., Cogley, J. G., Wouters, B., Arendt, A. A., Wahr, J., Berthier,
453 E., Hock, R., Pfeffer, W. T., Kaser, G., Ligtenberg, S. R. M., Bolch, T., Sharp, M. J.,
454 Hagen, J. O., van den Broeke, M. R., and Paul, F.: A Reconciled Estimate of
455 Glacier Contributions to Sea Level Rise: 2003 to 2009, *Science*, 340(6134),
456 852–857, doi:10.1126/science.1234532, 2013.
- 457 Goodwin, B. P.: Recent Environmental Changes on the Antarctic Peninsula as
458 Recorded in an ice core from the Bruce Plateau. PhD diss., The Ohio State
459 University, 247 pp., 2013.
- 460 Haran, T., Bohlander, J., Scambos, T. and Fahnestock, M.: MODIS Mosaic of Antarctica
461 2004 (MOA 2004) Image Map. Boulder, Colorado USA: National Snow and Ice
462 Data Center. <http://dx.doi.org/10.7265/N5ZK5DM5>, 2005, updated 2013.
- 463 Howat, I. M., Joughin, I., and Scambos, T. A.: Rapid Changes in Ice Discharge from
464 Greenland Outlet Glaciers, *Science*, 315(5818), 1559–1561, 2007.
- 465 Ivins, E. R., Watkins, M. M., Yuan, D.-N., Dietrich, R., Casassa, G., and Rülke, A.: On-
466 land ice loss and glacial isostatic adjustment at the Drake Passage: 2003–
467 2009, *J. Geophys. Res.-Earth*, 116, B02403, doi:10.1029/2010JB007607,
468 2011.
- 469 Joughin, I., Howat, I. M., Fahnestock, M., Smith, B., Krabill, W., Alley, R. B., Stern, H.,
470 and Truffer, M.: Continued evolution of Jakobshavn Isbrae following its rapid
471 speedup, *J. Geophys. Res.-Earth*, 113, F04006, doi:10.1029/2008JF001023,
472 2008.
- 473 Korona, J., Berthier, E., Bernard, M., Rémy, F., and Thouvenot, E.: SPIRIT. SPOT 5
474 stereoscopic survey of Polar Ice: Reference Images and Topographies during
475 the fourth International Polar Year (2007–2009), *ISPRS J. Photogramm.*, 64,
476 204–212, doi:10.1016/j.isprsjprs.2008.10.005, 2009.

- 477 Kunz, M., King, M. A., Mills, J. P., Miller, P. E., Fox, A. J., Vaughan, D. G., and Marsh, S.
478 H.: Multi-decadal glacier surface lowering in the Antarctic Peninsula,
479 *Geophys. Res. Lett.*, L19502, 10.1029/2012GL052823, 2012.
- 480 Lenaerts, J. T. M., van den Broeke, M. R., van de Berg, W. J., van Meijgaard, E., and
481 Munneke, P. K.: A new, high-resolution surface mass balance map of
482 Antarctica (1979-2010) based on regional atmospheric climate modeling,
483 *Geophys. Res. Lett.*, 39, L04501, 4501–4501, doi:10.1029/2011GL050713,
484 2012.
- 485 Ligtenberg, S. R. M., Helsen, M. M., and van den Broeke, M. R.: An improved semi-
486 empirical model for the densification of Antarctic firn, *The Cryosphere*, 5(4),
487 809–819, doi:10.5194/tc-5-809-2011, 2011.
- 488 Luthcke, S. B., Sabaka, T. J., Loomis, B. D., Arendt, A. A., McCarthy, J. J., and Camp, J.:
489 Antarctica, Greenland and Gulf of Alaska land-ice evolution from an iterated
490 GRACE global mascon solution, *J. Glaciol.* 59, 613–631,
491 doi:10.3189/2013JoG12J147, 2013.
- 492 McMillan, M., Shepherd, A., Sundal, A., Briggs, K., Muir, A., Ridout, A., Hogg, A., and
493 Wingham, D.: Increased ice losses from Antarctica detected by CryoSat-2,
494 *Geophys. Res. Lett.* doi:10.1002/2014GL060111, 2014.
- 495 Mulvaney, R., Abram, N. J., Hindmarsh, R. C., Arrowsmith, C., Fleet, L., Triest, J., ... &
496 Foord, S.: Recent Antarctic Peninsula warming relative to Holocene climate
497 and ice-shelf history, *Nature* 489(7414), doi:10.1038/nature11391, 141-
498 144., 2012.
- 499 Nick, F. M., Vieli, A., Howat, I. M., and Joughin, I.: Large-scale changes in Greenland
500 outlet glacier dynamics triggered at the terminus, *Nature Geosci.*, 2(2), 110–
501 114, 2009.
- 502 Pfeffer, W. T.: A simple mechanism for irreversible tidewater glacier retreat, *J.*
503 *Geophys. Res.-Earth*, 112 (F3), F03S25, doi:10.1029/2006JF000590, 2007.
- 504 Potocki, M., Mayewski, P. A., Kurbatov, A., Handley, M., Simoes, J. C., and Jaña, R.:
505 Detailed glaciochemical records from a northern Antarctic Peninsula site-
506 Detroit Plateau. In *AGU Fall Meeting Abstracts*, 1, p. 1822, 2011.
- 507 Pritchard, H. D., and Vaughan, D. G.: Widespread acceleration of tidewater glaciers
508 on the Antarctic Peninsula, *J Geophys Res-Earth*, 112(F3), F03S29,
509 doi:10.1029/2006JF000597, 2007.
- 510 Pritchard, H. D., Arthern, R. J., Vaughan, D. G., and Edwards, L. A.: Extensive dynamic
511 thinning on the margins of the Greenland and Antarctic ice sheets, *Nature*,
512 461(7266), 971–975, 2009.

- 513 Pritchard, H. D., Ligtenberg, S. R. M., Fricker, H. A., Vaughan, D. G., van den Broeke, M.
514 R., and Padman, L.: Antarctic ice-sheet loss driven by basal melting of ice
515 shelves, *Nature*, 484(7395), 502–505, doi:10.1038/nature10968, 2012.
- 516 Rignot, E., Casassa, G., Gogineni, P., Krabill, W., Rivera, A., and Thomas, R.:
517 Accelerated ice discharge from the Antarctic Peninsula following the collapse
518 of Larsen B ice shelf, *Geophys. Res. Lett.*, 31(18), 2004.
- 519 Rignot, E., Bamber, J. L., van den Broeke, M. R., Davis, C., Li, Y. H., van de Berg, J., and
520 van Meijgaard, E.: Recent Antarctic ice mass loss from radar interferometry
521 and regional climate modelling, *Nat. Geosci.*, 1(2), 106–110,
522 doi:10.1038/ngeo102, 2008.
- 523 Rott, H., Müller, F., Nagler, T., and Floricioiu, D.: The imbalance of glaciers after
524 disintegration of Larsen B ice shelf, Antarctic Peninsula, *The Cryosphere*,
525 5(1), 125–134, doi:10.5194/tc-5-125-2011, 2011.
- 526 Saha, S. et al.: The NCEP Climate Forecast System Reanalysis, *Bull. Amer. Meteor.*
527 *Soc.*, 91(8), 1015–1057, doi:10.1175/2010BAMS3001.1, 2010.
- 528 Sasgen, I., H. Konrad, E. R. Ivins, M. R. Van den Broeke, J. L. Bamber, Z. Martinec, and
529 V. Klemann (2013), Antarctic ice-mass balance 2003 to 2012: regional
530 reanalysis of GRACE satellite gravimetry measurements with improved
531 estimate of glacial-isostatic adjustment based on GPS uplift rates, *The*
532 *Cryosphere*, 7(5), 1499–1512, doi:10.5194/tc-7-1499-2013, 2013.
- 533 Scambos, T. A., Haran, T. M., Fahnestock, M. A., Painter, T. H., and Bohlander, J.:
534 MODIS-based Mosaic of Antarctica (MOA) data sets: Continent-wide surface
535 morphology and snow grain size, *Remt. Sens. Environ.*, 111(2), 242-257,
536 2007.
- 537 Shepherd, A. et al.: A Reconciled Estimate of Ice-Sheet Mass Balance, *Science*,
538 338(6111), 1183–1189, doi:10.1126/science.1228102, 2012.
- 539 Shuman, C. A., Zwally, H. J., Schutz, B. E., Brenner, A. C., DiMarzio, J. P., Suchdeo, V. P.,
540 and Fricker, H. A.: ICESat Antarctic elevation data: preliminary precision and
541 accuracy assessment, *Geophys. Res. Lett.* 33(7), doi:
542 10.1029/2005GL025227, 2007.
- 543 Shuman, C. A., Berthier, E., and Scambos, T. A.: 2001-2009 elevation and mass losses
544 in the Larsen A and B embayments, Antarctic Peninsula, *J. Glaciol.*, 57(204),
545 737–754, 2011.
- 546 Stammerjohn, S. E., D. G. Martinson, R. C. Smith, X. Yuan, and D. Rind, D.: Trends in
547 Antarctic annual sea ice retreat and advance and their relation to El Niño–
548 Southern Oscillation and Southern Annular Mode variability, *J. Geophys. Res.*
549 *Oceans* (1978–2012), 113(C3), doi: 10.1029/2007JC004269, 2008.

550 van den Broeke, M.,: Strong surface melting preceded collapse of Antarctic Peninsula
551 ice shelf, *Geophys. Res. Lett.*, 32(12), L12815, doi:10.1029/ 2005GL023247,
552 2005.

553 Zagorodnov, V., Nagornov, O., Scambos, T. A., A. Muto, A., Mosley-Thompson, E.,
554 Pettit, E. C., and Tyuflin, S.: Borehole temperatures reveal details of 20th
555 century warming at Bruce Plateau, Antarctic Peninsula, *The Cryosphere*, 6(3),
556 675–686, doi:10.5194/tc-6-675-2012, 2012.

557 Zgur, F., Rebesco, M., Domack, E. W., Leventer, A., Brachfeld, S., and Willmott,
558 V.:Geophysical survey of the thick, expanded sedimentary fill of the new-born
559 Crane fjord (former Larsen B Ice Shelf, Antarctica), US Geological Survey and
560 the National Academies; USGS OF-2007-1047, Extended Abstract 141, 2007.

561

562 **Table 1. Summary of Mass Balance for the northern Antarctic Peninsula, 2001-2010**
 563 Units: Area (km²), Mean dM/dt (Gt a⁻¹), Number of Measurements, Mean dh/dt (m a⁻¹), Mean dV/dt (km³ a⁻¹)

566 Region	Ice-Covered Area	Total dM/dt ^a	Ice Front Retreat				Below 1000 m a.s.l.					Above 1000 m a.s.l.			
			Area ^b	dh/dt ^c	dV/dt ^{d,h}	Area	dDEM ^e	ICESat ^f	dh/dt ^g	dV/dt ^h	Area	ICESat ^f	dh/dt ^g	dV/dt ^h	
567 nAP <66°S, 1-33	34232.8	-24.9	325.6	-3.5	-1.2	23582.6	44.8	12476	-1.00	-23.1	10651.7	2668	-0.31	-3.4	
568 nAP West, 1-11	14338.2	-4.8	7.8	-5.3	-0.2	9014.3	38.6	2999	-0.27	-2.4	5323.7	893	-0.59	-2.8	
569 nAP North, 12-14	3688.0	-2.4	4.0	-3.3	-0.1	3684.3	8.2	2204	-0.69	-2.5	3.7	(0)	(-0.31)	0.0	
570 nAP East, 15-33	16207.5	-17.7	313.8	-5.7	-0.9	10884.0	62.4	7279	-1.67	-18.2	5323.5	1775	-0.10	-0.6	
571 Northwest AP Coast ⁱ	5255.1	-1.7	--	--	--	3417.9	35.1	1270	-0.27	0.9	1837.0	575	-0.50	-0.9	
572 Western IFL Glaciers ^j	679.4	-1.1	11.8	-4.6	-0.03	452.1	35.6	450	-2.24	-1.0	226.5	(0)	(-0.84)	-0.2	
573 Eastern ISL Glaciers ^k	9262.3	-15.0	305.7	-5.9	-0.90	6030.9	70.9	3903	-2.60	-15.7	3232.6	941	-0.01	-0.2	
574 James Ross Island ^l	1800.8	-2.4	47.1	-3.3	-0.08	1380.0	58.0	417	-1.93	-2.7	420.7	215	0.02	0.0	
575 Prince Gustav tributaries ^m	1885.0	-2.7	58.2	-3.6	-0.10	1478.4	76.6	475	-2.03	-3.0	406.7	123	0.23	0.1	
576 Larsen A tributaries ⁿ	3184.4	-4.9	29.3	-2.7	-0.04	2094.8	85.5	1594	-2.32	-4.9	1089.7	329	-0.08	-0.1	
577 Larsen B ISL tributaries ^o	4192.9	-7.9	218.2	-3.9	-0.82	2457.7	55.2	1834	-3.18	-7.8	1736.2	489	-0.13	-0.2	
578 Scar Inlet Ice Shelf trib. ^p	3524.5	-1.4	--	--	--	2089.8	46.4	1965	-0.47	-0.7	1434.7	715	-0.37	-0.5	

579 Abbreviations for place names: nAP, northern Antarctic Peninsula; ISL, ice shelf loss; IFL, ice front loss.
 580 ^aAssuming mean density of 900 kg/m³ for all dV/dt measurements. Errors for these values are 0.9 times the sum of errors for dV/dt for each row.
 581 ^bArea determined from additional ASTER, SPOT, and Landsat images, spanning 2000-2002 to 2009-2010
 582 ^cRate of elevation loss measured just above area of grounded ice retreat.
 583 ^dVolume loss assumes flotation was reached midway between 2001 – 2010 (period of observations).
 584 ^ePercent area covered by differential DEM satellite stereo-image data
 585 ^fNumber of repeat-track point measurements used. If <10 ICESat dh/dt measurements are available, the regional mean ICESat dh/dt for areas > 1000 m (-0.31 m a⁻¹) or, for sub-basins, the main basin mean, is used.
 586 ^gHypsometric weighting for areas below 1000 m elevation; weighted by number of ICESat measurements for areas above 1000 m elevation.
 587 ^hErrors on dV/dt can be determined by: ±0.3 m a⁻¹ * area for regions ≤1000 m a.s.l. (dDEM data) and ±0.15 ma⁻¹ * area for regions >1000 m a.s.l.
 588 ⁱGlacier basins 8 – 11
 589 ^jGlacier basins 1a, 4a, 6a, and 12a
 590 ^kGlacier basins 19, 21-25, 26b, 27-30, and 31a.
 591 ^lGlacier basins 17, 18, and 19
 592 ^mGlacier basins 19 and 21
 593 ⁿGlacier basins 22-25
 594 ^oGlacier basins 26b, 27-30, and 31a
 595 ^pGlacier basins 31b, 32, and 33

601 **Table 2. Comparison of total mass balance (dM/dt), input surface mass (dM_i/dt), and**
 602 **resulting imbalance ratio.**

603 Units: Area, km²; dM/dt, Gt a⁻¹; Mean dh/dt, m a⁻¹; SMB, kg m⁻² a⁻¹; dM_i/dt, Gt a⁻¹

604 Region	Ice-Covered Area	Total dM/dt	Mean dh/dt	Mean SMB	Total dM _i /dt	Imbal. ratio	<1000 dh/dt	<1000 SMB	<1000 dM _i /dt	<1000 ratio	>1000 dh/dt	>1000 SMB	>1000 dM _i /dt	>1000 ratio
605 nAP <66°S, 1-33	34232.8	-24.8	-0.77	1543	54.2	-0.45	-1.00	1295	29.9	-0.70	-0.31	2104	23.1	-0.18
606 nAP West, 1-11	14337.3	-4.6	-0.33	2112	30.4	-0.14	-0.27	1964	17.7	-0.12	-0.59	2361	12.6	-0.17
607 nAP North, 12-14	3688.0	-2.4	-0.69	537	2.0	-1.15	-0.69	537	2.0	-1.15	(-0.31)	920	0.0	--
608 nAP East, 15-33	16207.6	-17.8	-1.20	1268	21.8	-0.81	-1.75	1007	10.5	-1.56	-0.10	1844	9.8	-0.06
609 Northwest AP Coast ^a	5255.1	-1.7	-0.35	2012	10.6	-0.16	-0.27	1770	6.0	0.13	-0.51	2458	4.5	-0.18
610 Western IFL Glaciers ^b	679.4	-1.1	-1.77	1839	1.2	-1.26	-2.24	1484	0.7	-1.29	-0.83	2546	0.6	-0.28
611 Eastern ISL Glaciers ^c	9262.3	-15.0	-1.66	1399	13.0	-1.15	-2.60	1143	6.9	-2.05	-0.07	1898	6.1	-0.04
612 James Ross Island ^d	1800.8	-2.4	-1.44	689	1.2	-2.09	-1.93	653	0.9	-2.70	0.02	834	0.4	0.00
613 Prince Gustav tributaries ^e	1885.0	-2.7	-1.54	1173	2.2	-1.23	-2.03	968	1.4	-1.93	0.21	2003	0.8	0.10
614 Larsen A tributaries ^f	3184.4	-4.9	-1.55	1624	5.2	-0.94	-2.32	1358	2.8	-1.58	-0.08	2154	2.3	-0.03
615 Larsen B ISL tributaries ^g	4192.9	-7.9	-1.80	1329	5.6	-1.42	-3.18	1064	2.6	-2.68	-0.13	1713	3.0	-0.07
616 Scar Inlet Ice Shelf trib. ^h	3524.5	-1.4	-0.42	1296	4.6	-0.30	-0.47	787	1.6	-0.38	-0.37	2049	2.9	-0.16
617 ^a Glacier basins 8 – 11														
618 ^b Glacier basins 1a, 4a, 6a, and 12a														
619 ^c Glacier basins 19, 21-25, 26b, 27-30, and 31a														
620 ^d Glacier basins 17, 18, and 19														
621 ^e Glacier basins 19 and 21														
622 ^f Glacier basins 22-25														
623 ^g Glacier basins 26b, 27-30, and 31a														
624 ^h Glacier basins 31b, 32, and 33														

625
626

627 **Figures**

628

629 Figure 1. Location and outline of basins and sub-basins in the study area, and sites of
630 two climate ice cores discussed in the text. Region names, basin numbers, and
631 abbreviations are the same as in Table S2. Major drainage basins are outlined in
632 white, sub-basins are indicated in blue. Base image is the MODIS Mosaic of
633 Antarctica (Scambos et al., 2007).

634

635 Figure 2. Elevation change rates (dH/dt) and major and minor glacier basin or
636 islands for the northern Antarctic Peninsula study area. Cyan outlines indicate the
637 measured study basins and islands; surrounding numbers and letters refer to Table
638 1 entries. Magenta outlines with lower-case letter labels identify sub-basins areas
639 within the major basins where a separate hypsometric interpolation was used. Black
640 contour lines indicate 1000 m a.s.l. elevation. Major ice shelf retreat areas since
641 1980 (*Cook and Vaughan, 2010*) are indicated in grey-blue, with years of major
642 collapse events and the limit of extensive grounded ice loss shown. Ice edge is from
643 a 2009 MODIS mosaic (Haran et al., 2014).

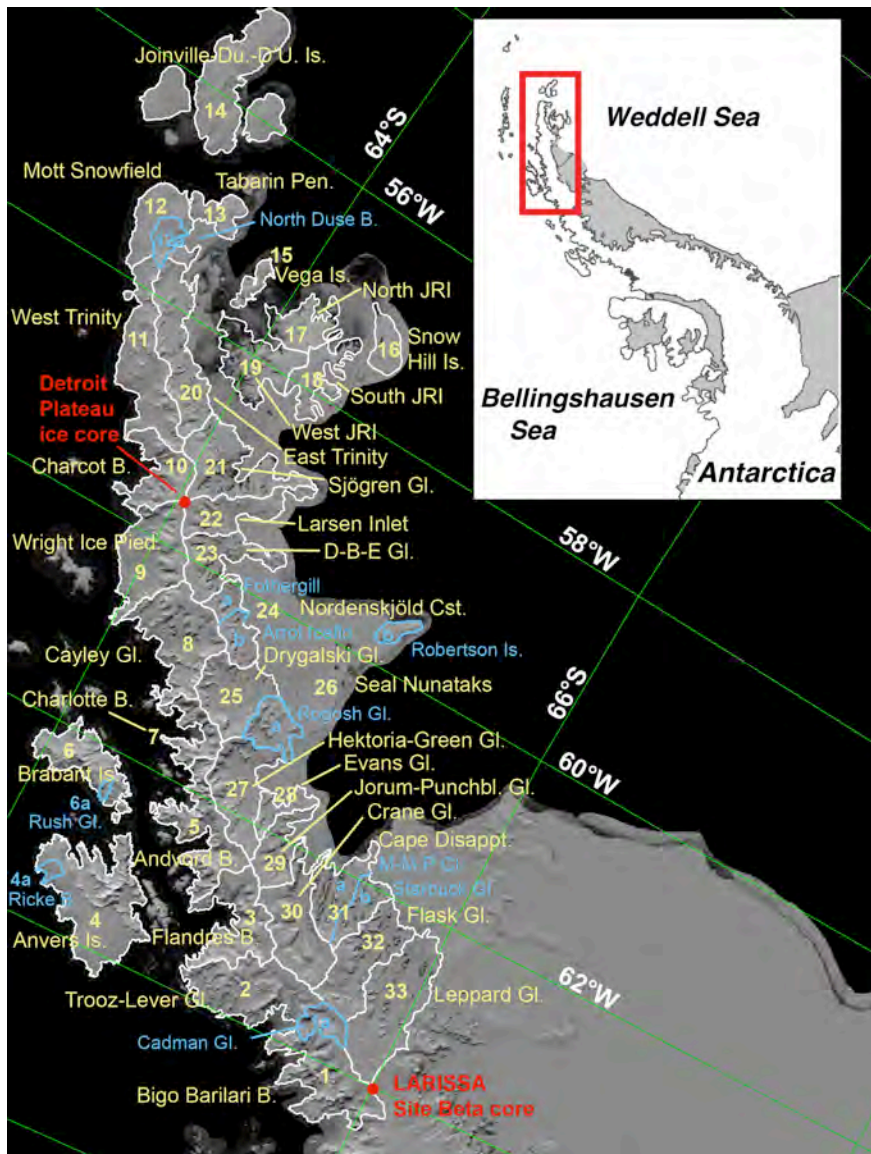
644

645 Figure 3 a-f. Hypsometry of elevation and volume changes of western basins (panel
646 a and b; basins 1 – 11 in Table 1), eastern basins with major ice shelf loss in the
647 period 1986 – 2009 (panels c and d; basins 19, 21-25, and 27-30 in Table 1), and
648 basins draining to the Scar Inlet ice shelf area (panels e and f; basins 31b, 32, and 33
649 in Table 1). Height is binned in 50 m intervals. Note that rates of elevation change
650 trends at the highest elevations (>2000 m a.s.l., right side of left column of panels)
651 are based on few data and are not reliable.

652

653 Figure 4. Comparison of the study area basin extents with RACMO-2 estimated SMB
654 in $\text{kg m}^{-2} \text{a}^{-1}$ (panel a) and mass imbalance ratio for the basin areas separated by
655 high and low elevation areas (above and below 1000 m; panel b).

656



657

658 **Figure 1.** Location and outline of basins and sub-basins in the study area, and sites of two
 659 climate ice cores discussed in the text. Region names, basin numbers, and abbreviations are
 660 the same as in Table B1. Major drainage basins are outlined in white, sub-basins are
 661 indicated in blue. Base image is the MODIS Mosaic of Antarctica (Scambos et al., 2007).

662

663

664

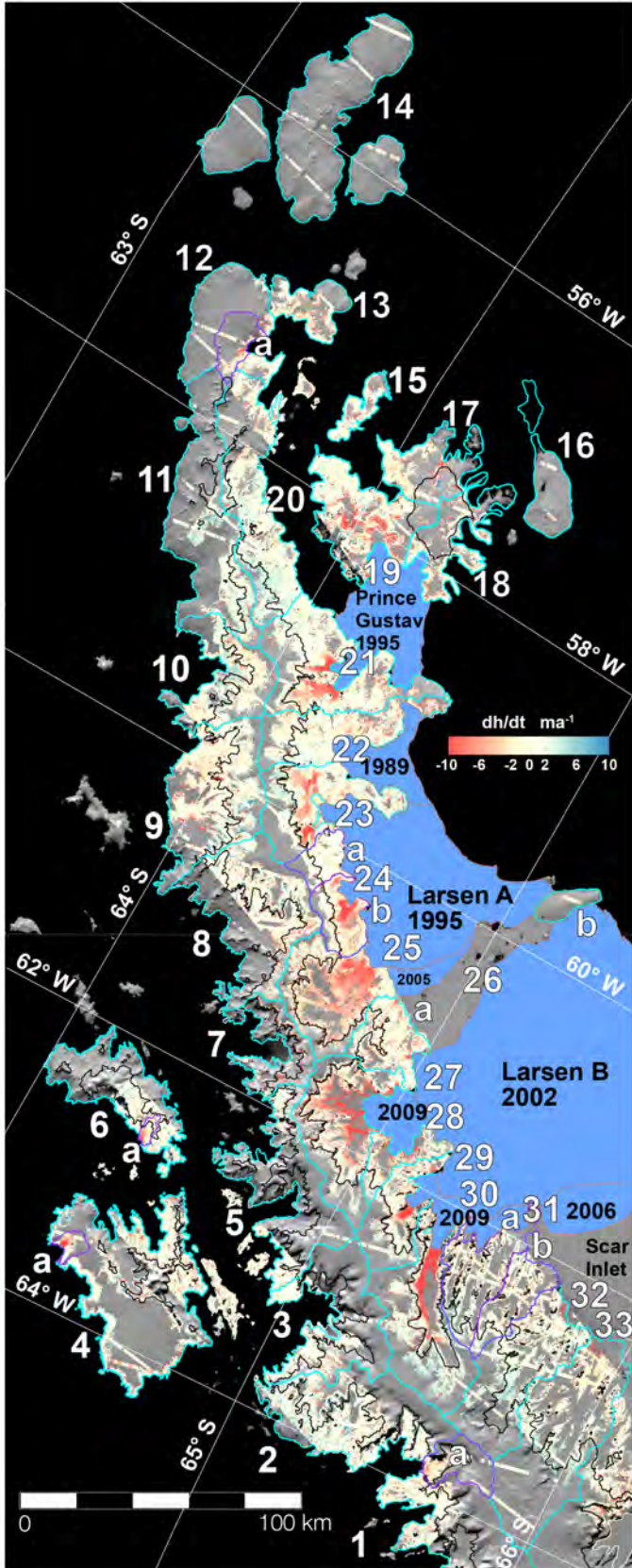
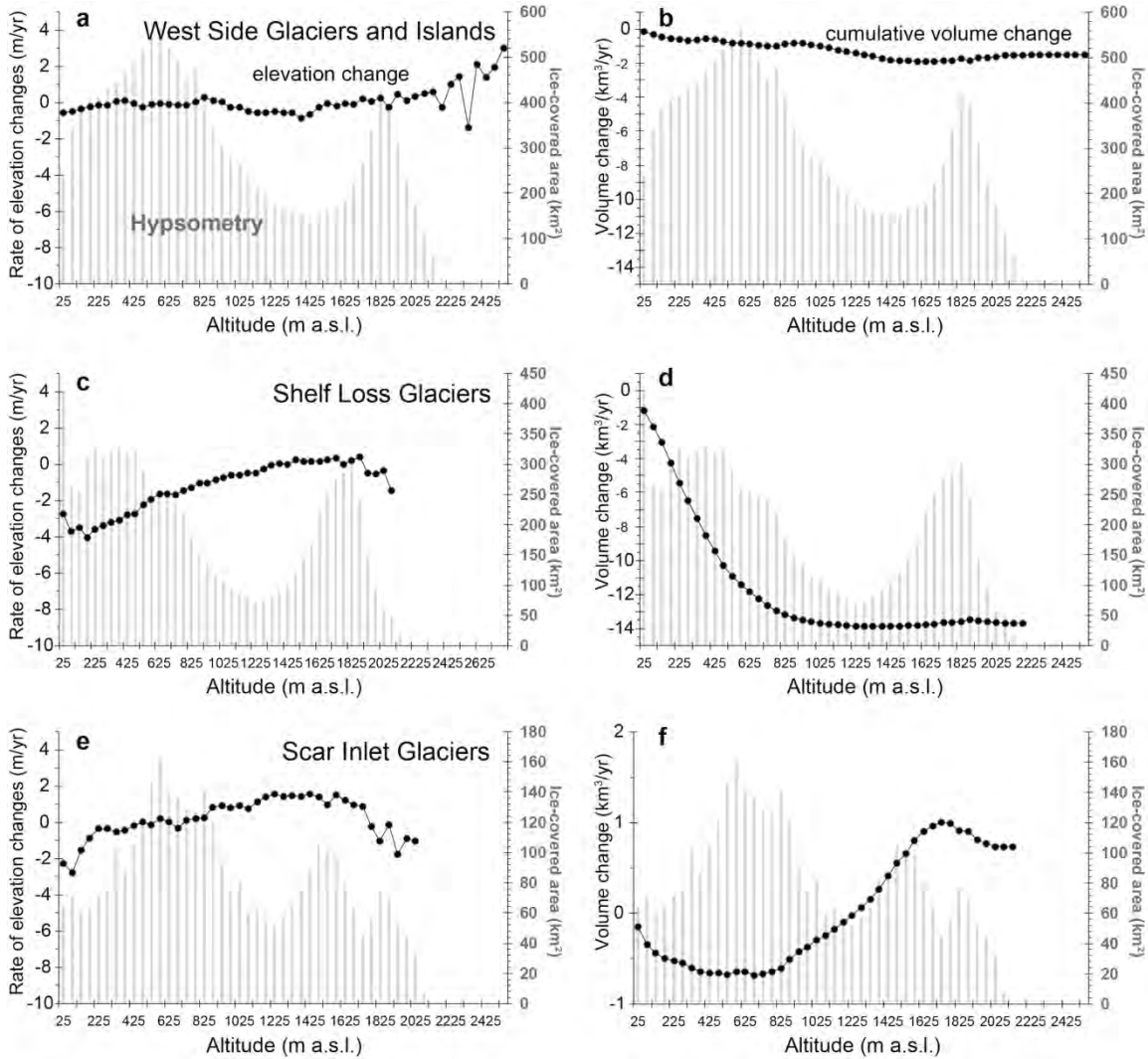


Figure 2. Elevation change rates (dh/dt) and major and minor glacier basin or islands for the northern Antarctic Peninsula study area. Cyan outlines indicate the measured study basins and islands; surrounding numbers and letters refer to Table 1 entries. Magenta outlines with lower-case letter labels identify sub-basins areas within the major basins where a separate hypsometric interpolation was used. Black contour lines indicate 1000 m a.s.l. elevation. Major ice shelf retreat areas since 1980 (*Cook and Vaughan, 2010*) are indicated in grey-blue, with years of major collapse events and the limit of extensive grounded ice loss shown. Ice edge is from a 2009 MODIS mosaic (*Haran et al., 2013*).

666
667
668
669
670

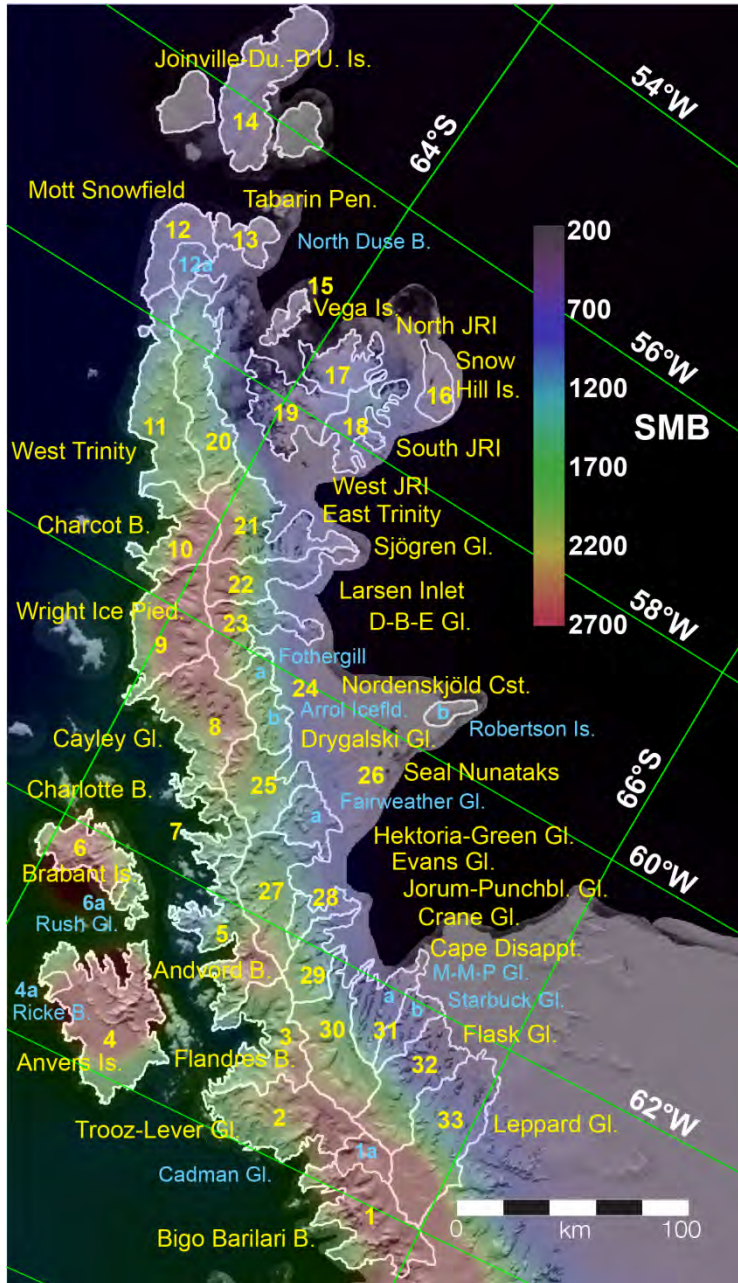


671
672
673
674
675
676

Figure 3 a-f. Hypsometry of elevation and volume changes of western basins (panel a and b; basins 1 – 11 in Table 1), eastern basins with major ice shelf loss in the period 1986 – 2009 (panels c and d; basins 19, 21-25, and 27-30 in Table 1 and B1), and basins draining to the Scar Inlet ice shelf area (panels e and f; basins 31b, 32, and 33 in Table 1 and S2). Height is binned in 50 m intervals. Note that rates of

677 elevation change trends at the highest elevations (>2000 m a.s.l., right side of left
678 column of panels) are based on few data and are not reliable.

679



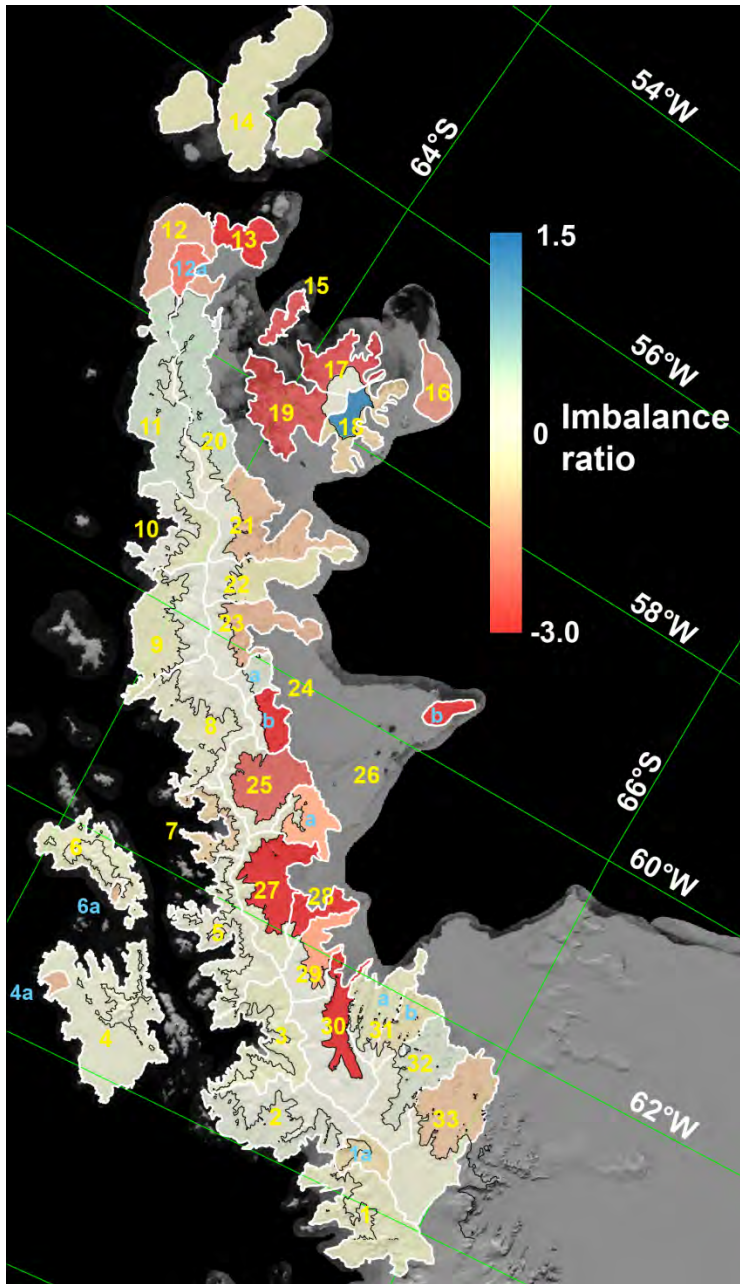
680

681 **Figure 4a.**

682 **Figure 4 a and b.** Comparison of the study area basin extents with RACMO-2
683 estimated SMB in $\text{kg m}^{-2} \text{a}^{-1}$ (a) and mass imbalance ratio for the basin areas
684 separated by high and low elevation areas (above and below 1000 m; b).

685

686



687

688 **Figure 4b**

689 **Figure 4 a and b.** Comparison of the study area basin extents with RACMO-2
690 estimated SMB in $\text{kg m}^{-2} \text{a}^{-1}$ (a) and mass imbalance ratio for the basin areas
691 separated by high and low elevation areas (above and below 1000 m; b).